UNIVERSITETET I AGDER

Control Design for Load Reduction on Wind Turbine System

BY

Ragnar Eide

Supervisor:
Prof. Hamid Reza Karimi(UiA)

This Master's Thesis is carried out as a part of the education at the University of Agder and is therefore approved as a part of this education.

University of Agder, 2011

Faculty of Engineering and Science

Department of Engineering

Abstract

The wind power industry is currently the fastest growing renewable energy sector throughout the world. This requires the technical expertise among engineers and researchers in the wind energy field to find technical solutions which do not slow down this process. Since the technology is being developed at such a rapid rate, the industry is facing many challenging problems, especially among systems and control researchers. To ensure an economically competitive wind power production, the trend is to increase the turbine size while at the same time minimize material usage. These factors result in increasing fatigue loads, which need to be accounted for by a well defined control design. In this work, the basic theories of wind turbines are reviewed firstly before proceeding with modeling, simulation, and controls implementation. What is suggested as a means of load reduction is firstly a Disturbance Accommodating Control (DAC) approach. This is then compared with the well-known Linear Quadratic Gaussian (LQG) controlling method. To improve the robustness of the LQG, an additional Loop Transfer Recovery (LTR) procedure will be implemented and compared with the results from the LQG. The main focus in this work is to use these modern control theories to reduce the torque variations by using speed control with collective blade pitch adjustments. Simulations show that better load reduction can be obtained by the dynamic compensator extracted from the LTR procedure than with a regular LQG regulator.

Acknowledgments

This report comprises the results from the graduation project at University of Agder. The thesis has been carried out based on a problem description suggested by the University, and is a part of the requirement for obtaining the degree of Master of Science in Mechatronics.

To be able to come to an end in this project and present the results in this report, I would like to thank prof. Hamid Reza Karimi for his supervision and for coming up with the first ideas of this assignment. I would also like to acknowledge the Mechatronics group at the University for giving me the opportunity to work on such an interesting project. I would also like to acknowledge the support provided by other students who have all inspired this work, and prof. Anne Mueller for helpful inputs on the report writing. Finally I would like to thank my wife for her patience throughout this semester.

Contents

Chapter 1

Introduction

1.1 Background and Motivation

The world's energy consumption from the beginning of the industrial revolution in the 18 th. century and until today has increased at a tremendous degree. Since a large part of the energy has come from sources like oil and coal have the negative impacts on the environment increased proportionally. Therefore, more sustainable and climate friendly energy production methods are emphasized among researchers and environmentalists throughout the world. This is the reason why renewable energies, and wind power particularly, have now become an essential part of the energy programs for most of governments all over the world. One example is seen by the outcome of the European Conference for Renewable Energy in Berlin in 2007 where EU countries defined ambitious goals when it comes to the increase in use of renewable energy resources. One of the goals was that by 2020, the EU would seek to get 20% of energy consumption from renewable energies [30].

Wind power, in conjunction with other renewable power production methods, has been suggested to play a more and more important role in the future power supply [58] and [43]. One of the reasons for these expectations is the enormous available potential when it comes to wind resources. One of the most comprehensive study on this topic [4] found the potential of wind power on land and near-shore to be 72TW, which alone could have provided over five times the world's current energy use in all forms averaged over a year.

The World Wind Energy Association (WWEA) estimates the wind power investment worldwide to expand from approximately 160 GW installed capacity at the end of 2010 to 1900 GW installed capacity by 2020 [6]. One example is from the USA, where the current contribution of electricity from wind power is merely 1,8% (2009) [5]. However, the U.S Department of Energy is now laying a framework to get as much as 20% contribution by the year 2030.

Due to the economical advantages of installing larger wind turbines (WTs), the typical size of utility-scale turbines has grown dramatically over the last three decades. In addition to the increasing turbine-sizes, cost reduction demands imply use of lighter and hence more flexible structures. If the energy-price from WTs in the coming years are to be competitive with other power production methods, an optimal balance must be made between maximum power capture on one side, and load-reduction capability on the other side. To be able to obtain this is a well defined control-design needed to improve energy capture and reduce dynamic loads. This combined with the fact that maintenance and constant supervision of WTs at offshore locations

is expensive and very difficult, which has further increased the need of a reliable control system for fatigue and load reduction. New advanced control approaches must be designed such as to achieve to the 20- to 25-year operational life required by today's machines [60].

Presented in this report is an above rated wind speed (Region III) regulation of a Horizontal Axis Wind Turbine (HAWT). The first method applied is Disturbance Accommodating Control (DAC) which is compared to the LQG controller. The LQG will then be extended by using the so-called Loop Transfer Recovery (LTR) method for improving the robustness properties. The LTR method is shown to meet the requirements for good load mitigation by utilizing a dynamic controller extracted from the LTR algorithm provided with the Robust Control Toolbox in MATLAB.

1.2 Problem Formulation and Limitations

A WT is often put in an unfriendly environment, especially when the wind conditions is concerned. The wind will cause large dynamic loads, especially on the blades and the blade joints [56]. The only way to modify the dynamic behavior of the WT is by actively or passively control the turbine.

Let's first consider a WT operated at rated speed. A rise in the mean wind speed may necessarily cause the force on the rotor blades to increase, and hence the torque to rise as well. If the generator is allowed to accelerate will this situation result in increased rotor speed if no control is utilized to interact the change in wind speed. This is not a desired situation when the matter of fatigue is concerned, since this variations in torque will give stress cycles, which in turn will reduce the lifetime of the WT components. Hence, the design of a control system capable of mitigating the loads by using speed control for above rated wind speeds are the focus of this project. It is important to note that only changes in the mean wind speed is considered here, and not the turbulent and stochastic properties.

One especially important issue when considering fatigue is the large torque variations at the generator's shaft due to the high inertia of the turbine versus wind speed variations when using a control scheme based exclusively on the steady-state optimization. This could lead to fatigue damage in the mechanical subsystems, such as the gear-box. To account for this one may set up a combined optimization criterion which aims at *maximizing*of the energy conversion and *minimizing* the torque variations. This approach has been used by Ekelund in his PhD thesis [24] and later in the works of Munteanu et. al. (see [29]). It is important to note that if optimality should have been treated in this work, it would have been necessary to perform a trade-off between the energy conversion maximization and the control input minimization. However, although this is a very crucial topic when designing control systems, optimality considerations has not been within the scope of this project, and hence no such trade-off is considered here.

1.3 Outline

Chapter 2 is meant to give a theoretical foundation of the further discussion in subsequent chapters. Firstly are WT energy conversion viewed form an aerodynamic perspective by a description of the Elementary Momentum Theory and the aerodynamic lift and drag coefficients. Following this is a short overview of the Blade Element Momentum Theory. The principles of operation of a WT are then explained, followed by a description of the main elements of a WT. Finally, the issue of fatigue and a description of the state space representation is presented.

Chapter 3 will be devoted to the modeling phase. The aim is to come up with a simplified state space model of the WT appropriate to be used in the control design in the subsequent chapters.

The control system design is covered in Chapter 4. After a historical overview and a state-of-the-art presentation of WT control are the elements involved in the practical control designed merged with a theoretical description of each topic.

The model will then be implemented into a simulation model in the in the MATLAB/Simulink environment in Chapter 5, where the DAC theory is first introduced followed by LQG control. The results from the LQG will then be compared with results when using the LTR control synthesis to see whether the latter can be regarded as a solution to meet the specified goal of load mitigation. Finally, the conclusions and further improvement suggestions are drawn in Chapter 6.

Chapter 2

The Wind Turbine System

2.1 Introduction

In the first section in this chapter will some fundamental aspects of WT power conversion be presented. This is done by the Elementary Momentum Theory (EMT) which is followed by an explanation of the essential lift and drag coefficients. Following this will the Blade Element Momentum (BEM) theory be described, which is a model frequently used in blade-performance calculations and blade design [36]. Then, after a short description of operation principles, WT components and most important categories of loads, some issues regarding fatigue are described at the end.

2.2 Wind Energy Conversion Principles

The most fundamental relationship when considering WT power production is the rotor's dependency of the power available in the wind approaching the blades. The power in the wind in steady state can be described mathematically according to the following equation

$$P_w = 0.5\rho\pi R^2 V^3 \tag{2.1}$$

where ρ is the air density, R is the radius of the swept area of the blades, and V is the wind speed.

The Elementary Momentum Theory (EMT), also known as the Disk Actuator Theory, is a relatively simple way of explaining the physics behind the conversion of kinetic energy in the wind into mechanical torque. Since the shape of the converter is irrelevant when using EMT, the model's field of application in WT design and control is therefore very limited. However, it describes some crucial rules and properties and will be included by way of introduction.

The method can be traced back to Rankine (1865) and Froude (1885) [34], who developed models to predict propeller performances. Albert Betz (1920) then extended their work also to the application of the theory on a turbine rotor. Betz found that an air stream passing through a given cross sectional area is restricted to a certain fixed portion of the energy contained in the air stream [34]. He also found a relationship between the optimal power extraction and the relative velocity between free stream velocity and the velocity far behind the converter.

EMT is based on some basic assumptions (see [34] for details) and assumes a control volume in which the boundaries are the surface of a stream tube and two cross sections of the stream tube. By applying the conservation of momentum to the control volume, one can find the net force on the contents of the volume. This force is according to Newtons Third Law equal and opposite to the thrust force from the wind on the WT. From the law of conservation of linear momentum, which states that the total momentum of a closed system of objects is constant, the thrust must be equal and opposite to the rate of change of momentum in the air stream. After applying the *Bernoulli Equation* on both sides of the rotor disk placed inside the control volume, the power extracted from the wind by the rotor can be expressed as the thrust multiplied by the wind velocity yielding to the equation for the power given as

$$P = \frac{1}{2}\rho A_r V^3 4a(1-a)^2 \tag{2.2}$$

where ρA_r is now the swept area, and a is the axial *induction factor* defined as the fractional decrease in the wind velocity between the free stream and the rotor plane.

Now, two important parameters regarding turbine performance are the *power coefficient*, C_P, and the *thrust coefficient*, C_T. The power coefficient is the ratio between the rotor power and the power in the wind given as

$$C_P = \frac{P}{\frac{1}{2}\rho V^3 A} = \frac{\frac{1}{2}\rho A_r V^3 4a(1-a)^2}{\frac{1}{2}\rho V^3 A} = 4a(1-a)^2 \tag{2.3}$$

It can be shown [34] that by taking the derivative of C_P and equal it to zero, the maximum power coefficient, $C_{P,max}$, is equal to 0.5926 [23] at $a = 1/3$. This value of the maximum theoretical power coefficient is called the *Betz limit* and denotes the maximum percentage of the energy in wind the rotor is able to extract. As already mentioned is this simple model only valid under certain assumptions. If one or more of these are violated, which is the case in practice, the Betz limit will be decreased accordingly.

Until now, the rotor has only been considered to be a disk with infinite number of blades. This assumption is of course useless when a practical application is concerned. The next section will therefore go on and discuss some crucial topics regarding WT energy conversion when also the geometry of the blades is taken into account. These principles will then relate the geometric shape of the blades with the mechanical torque of the WT.

2.3 WT Aerodynamics

2.3.1 Introduction

As showed in e.g [44], do WT aerodynamics exhibit phenomena that are rarely seen in other aerodynamic fields. Hence, to derive mathematical models to describe the aerodynamic properties is not at all an easy task. The topics in ongoing research clearly reflects the huge effort that is being laid down to develop reliable analysis and design tools [44]. An in-depth study of these topics is not within the scope of this work (please refer to [23] or [33] for this). However, as a starting point, and since it is important to understand the fundamental ideas of aerodynamics before coming to the control part will this topic be given relatively much space.

2.3.2 The Aerodynamic Lift and Drag Coefficients

The amount of energy the WT is able to extract from the air is governed by the aerodynamic properties of the blades, and is determined by the velocity and load distribution along the blades. Hence, an understanding of the motion of air (called a flow field) around the WT rotor enables the calculation of forces and moments that will be present at different locations for a given wind speed. This knowledge enables the WT designers to get an understanding of how much energy the turbine can extract from the air, and further; how the structural loads on the different parts of the turbine will be.

In general, the wind can be considered as a combination of a mean wind and turbulent fluctuations about a mean flow. Although the fluctuations in the wind is important when considering fatigue loads, experience has shown that the main aspects of the WT performance (mean power and mean loads) are determined by the aerodynamic forces generated by the mean wind [46]. With this background, merely the mean wind, yielding a steady state nature of the aerodynamics, is considered in this work. To further simplify, only a two dimensional flow will be considered.

The WT blades are shaped as an airfoil in the same way as an aircraft wing. Figure 2.1 depicts a 2D airfoil with the most important parameters. These parameters will be described in the following.

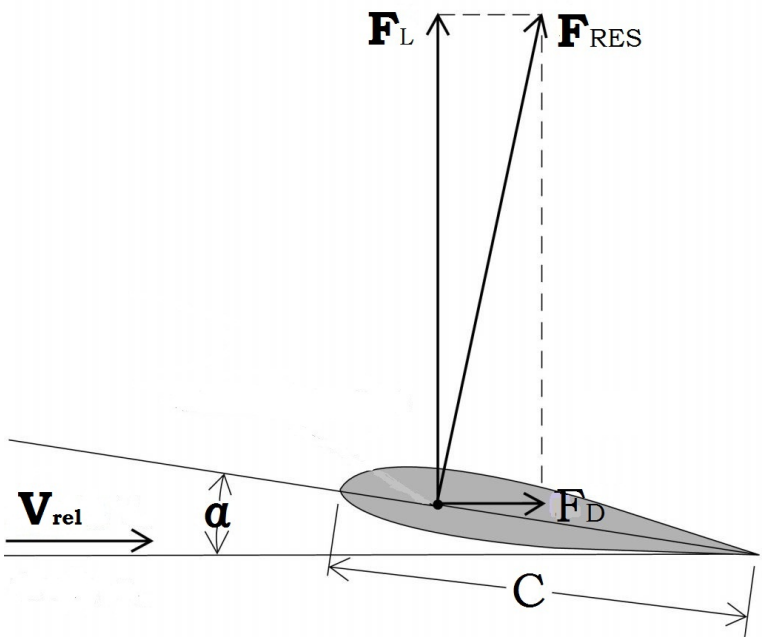

Figure 2.1: WT airfoil with resultant forces

Air flow over an airfoil-shaped blade produces a distribution of forces over the surface of the blade. It can be shown that there are only two basic sources of this aerodynamic force. The first is the pressure distribution along the surface of the blade, having its resultant given as F_L in Figure 2.1. The pressure exerted by the air at a point on the surface always acts perpendicular to the surface at that point. The resultant of this force is defined as perpendicular to the direction of the oncoming air flow (given as V_{rel} in Figure 2.1). This force is the *lift force* and the magnitude of this force is dependent on the corresponding *lift coefficient* defined as

$$C_L = \frac{F_L}{0.5A\rho V_{rel}^2 c} \tag{2.4}$$

where F_L is the lift force, ρ is the density of the wind, V_{rel} is the relative wind velocity approaching the

turbine, and$c$ is the cord length.

The second source of the aerodynamic force acting on the blade is due to the friction of the air against the surface. This force acts tangentially to the surface at that point and has a resultant force, the *drag force* (given as F_D in Figure 2.1). The corresponding *drag coefficient* is given as

$$C_D = \frac{F_D}{0.5A\rho V_{rel}^2 c} \tag{2.5}$$

The amount of surface area available for the oncoming wind is a key parameter when considering aerodynamic forces on the rotor blades. The angle at which the blade is adjusted (or pitched) is referred to as the *angle of attack*, denoted as α in Figure 2.1. A typical variation of lift and drag coefficients as functions of α is shown in Figure 2.2. As can be seen from this figure does the maximum lift coefficient occur at approximately 17°. It can be shown that the ratio between the lift and drag, C_L/C_D, where a maximum is reached, denoted by $(C_L/C_D)_{max}$, is present at a relatively low α. Beyond this angle does the lift force decreases with increasing α. From this we can see that we are able to control the angle of attack by pitching the blades, we also have a way to control the power of the turbine. This is the reason why the pitch angle, often denoted by β, will be used in the following as the control input for the sake of load mitigation.

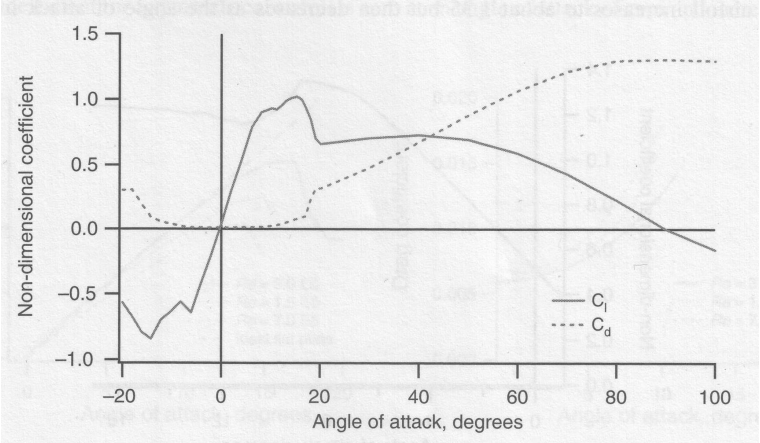

Figure 2.2: Typical curve for lift and drag coefficients as functions of angle of attack for a WT airfoil [46]

The peak of the lift coefficient curve, and the sudden change at approximately α = 17-18°, is due to flow separation from suction side of the airfoil and is called (dynamic) *stall effect*. Stall is understood as a situation which occurs when the angle of attack becomes so large that the air flow no longer can flow smoothly, or laminar, across the profile [55]. Air looses contact with the rear side of the blade, and strong turbulence occurs. Stalling was earlier used as a passive control of the WT to limit the velocity of the rotors at wind speeds above rated, i.e when the turbine produces maximum power. This passive stall regulation was done by shaping the blade such that an increase in the angle of attack occurs as the blades speed up above a certain level. However, a situation of stalling is not wanted for operating conditions below rated since this will decrease the amount of energy extracted from the wind.

To realize how the geometry now is taken into consideration can be shown through the overall power coefficient, which is given as the following integral (see [46] for more details)

$$C_P = \frac{8}{\lambda^2}\int_{\lambda_h}^{\lambda} a'(1-a)[1-(C_D/C_L)cot\phi]\, d\lambda_r \tag{2.6}$$

where λ is the tip speed ratio given as $\omega_r R/V$, with ω_r as denoting the rotor rotational speed, and λ_h is the local speed ratio at the hub. The difference between this expression and the one already given by EMT in Section 2.2 (cf. Eqn. (2.3)), is that now is the geometric shape taken into account through the lift and drag coefficients. It is therefore necessary to express C_P as an integral which must be evaluated in order to know the right value of the coefficients.

What is left on the discussion of WT aerodynamics is to describe the Blade Element Momentum (BEM) Theory. The beauty of this model is how it in a relative simple way can be used to predict forces and moments which is likely to occur for a given operation condition.

2.3.3 Blade Element Momentum Theory

The BEM theory is one of the oldest and most commonly used methods for calculating induced velocities on WT blades [48]. For instance, popular computer codes such as WT_{Perf} and *AeroDyn*, are using this model in their torque and force calculations. The reason for its popularity can be traced back to how the model treats rather complex issues in a relatively simple way, and hence does it require low computational power [46].

The BEM theory is based on the results from the EMT described in Section 2.2, but it goes beyond this theory by also considering the blade geometry. Hence BEM can be considered as a merging of EMT with the so-called *Blade Element Theory* (BET), which analyzes the forces at a section of the blade as a function of the blade geometry[1].

Based on the definitions of the lift and drag coefficients defined in Section 2.3.2 can the incremental normal force and torque be given as

$$dF_N = B\frac{1}{2}\rho V_{rel}^2(C_L cos\phi + C_D sin\phi)cdr \tag{2.7}$$

$$dQ = BrdF_T = Br\frac{1}{2}\rho V_{rel}^2(C_L sin\phi - C_D cos\phi)cdr \tag{2.8}$$

where in the first equation the incremental normal force dF_N is defined on the section a radius r in terms of number of blades, B, the relative wind velocity approaching the turbine, V_{rel}, with an angle ϕ, and the geometrical properties given by the lift and drag coefficients C_L and C_D. The second equation expresses the incremental torque in terms of the incremental tangential force to the circle swept by the rotor, dF_T, i.e the force which produces "useful" torque.

Now, from the EMT, the following two expressions for the differential torque and thrust can be obtained (cf. Section 2.2, with reference to [33] and [23])

$$dQ = 4a'(1-a)\rho V\omega_r r^3\pi dr \tag{2.9}$$

$$dF_N = 4a(1-a)\rho V^2\pi r dr \tag{2.10}$$

These expressions can be equated with dQ and dF_N from BET (cf. Eqns. (2.7) and (2.8)). Then, after some algebraic manipulations, is the lift coefficient, C_L, expressed in terms of the flow angle and the local speed

[1] Please refer to [33] or [23] for more details of this theory.

in the following way

$$C_L = 4sin\phi \left[\frac{(cos\phi - \lambda_r sin\phi}{\sigma'(sin\phi + \lambda_r cos\phi)} \right] \tag{2.11}$$

It is also useful to express the angular induction factor in terms of C_L and ϕ:

$$a' = \frac{1}{\left[\frac{4cos\phi}{(\sigma' C_L)} - 1 \right]} \tag{2.12}$$

The axial induction factor a can be expressed in terms of C_L and the flow angle ϕ

$$a = \frac{1}{\left[1 + \frac{4sin^2\phi}{(\sigma' C_L cos\phi)} \right]} \tag{2.13}$$

Eqns. (2.11) to (2.13) must now be solved to find the flow conditions and forces at each blade section. One method is to solve for C_L and the angle of attack, α. It can be shown from geometric considerations that there are two unknowns at each section of the blade, C_L and α. These can be found from empirical data given for the airfoil. When C_L and α have been found, a and a' can be found as well, using the Eqns (2.12) and (2.13). Now, by having these parameters, the power coefficient can be calculated.

The largest sources of error in power prediction from BEM have been traced back to errors in the airfoil lift and drag data, errors that in many cases have disregarded BEM as a valid model [46]. Also when the designer wants to include effects as yawed flow and unsteady aerodynamics, one must either incorporate these into the BEM analysis or use other methods, such as for instance vortex wake methods. For a more detailed discussion of strengths and limitations of the BEM theory, please refer to [48].

2.4 Operating Principles

Most utility-scale wind turbines in commercial use today are built according to the so-called Danish concept [20]. This turbine configuration consists of a horizontal axis rotor, a three-bladed actively pitched rotor in upwind orientation, and an active yaw system. In this work is this the only WT configuration treated[2]. But why are variable speed and pitch regulation preferred rather than the earlier more simple and robust concepts? Recalling from Section 2.2, how the power-coefficient, C_P, was defined as the ratio of extracted power divided by available power in the wind. It can be further showed that C_P is a function of the already mentioned tip speed ratio $\lambda = \omega_r R/V$, the pitch ratio β, as well as the wind speed V. A plot of C_P for a different values of β is depicted in Figure 3.2. (It is important to note that C_P in fact are given by complicated measurements and calculations based on geometric and experimental data, which shall not be discussed further here. However, when assuming quasi-stationarity, i.e a steady-state mass flow, the coefficients can be regarded as functions of β, λ, and V).

According to the plot in Figure 3.2, does C_P have a maximum at approximately $\lambda = 8$. The pitch angle β is for this curve zero[3]. Hence, any deviations from $\beta = 0$ will reduce the power capture. The advantages of a variable speed WT compared to a fixed speed turbine can easily be understood with this background. A variable speed WT can, when properly adjusted according to the wind speed, potentially operate with

[2] Yaw control is not covered in this project and only collective pitch control.
[3] Having $\beta = 0$ is an idealized case, and is not possible in real-life

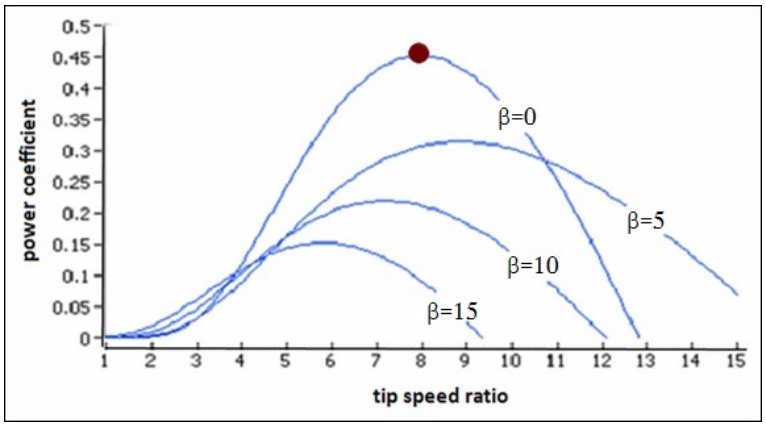

Figure 2.3: Plots of the power coefficients for different values of pitch angle β [37]

maximum efficiency over a wide wind speed range. By commanding constant generator torque, and setting blade pitch, the variable-speed turbine's rotor inertia prohibits rapid speed variations, and hence, a slower bandwidth pitch system can be used [60]. Obviously, a fixed-speed turbines cannot regulate the rotor speed and must rely on the aerodynamic design and additional blade pitch regulation to obtain constant, or rated, aerodynamic torque. In contrast, fixed-speed machines either suffer power spikes caused by rapid inflow velocity changes or pitch at high rates to cancel inflow changes.

2.4.1 Operating Regions

Typically, one may distinguish between three main modes of operation [21] according to three different wind speed regions. In the first region (Region I), the WT is not operating at all. It has its upper limit set to a certain threshold called cut-in speed (see Figure 2.4), which is usually around 3.5 m/s.

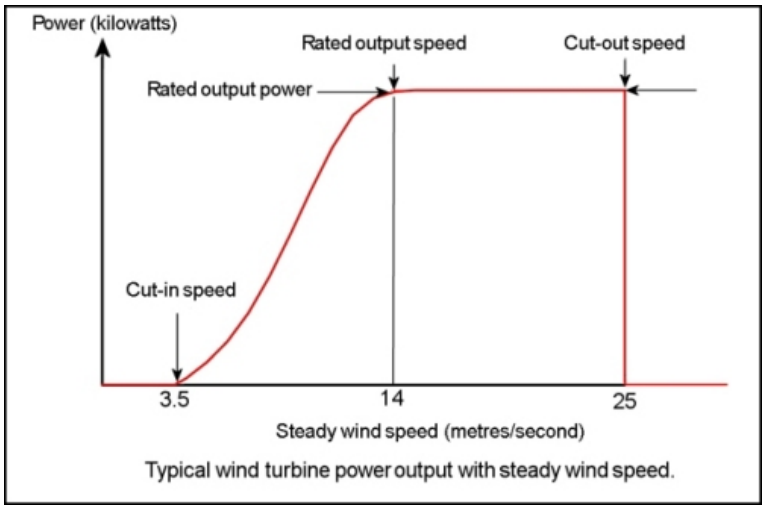

Figure 2.4: Example of power curve showing output power as a function of wind speeds [31]

Above the cut-in wind speed, the WT is connected to the grid and the rotor starts to rotate. The WT is now operating in Region II, and since it is desirable to extract as much energy as possible from the wind, the generator must be operated at maximum power coefficient. This means that the WT must be controlled so as to maintain a constant tip speed ratio for varying wind speeds. Hence, as the wind increases, the rotor

angular speed also increases correspondingly. This regulation policy is obtained by keeping the blade pitch setting fixed at the value of maximum power coefficient. By regulating the electrical torque the optimal rotor speed can thus be obtained. As can be seen from Eqn. (2.1), does the generated power increase according to a cubic law with increasing wind speed. Hence, the adjustment of the rotational speed can enable the turbine to be operated at its highest level of aerodynamic efficiency at a wide range of wind speeds.

In the last region (Region III), is the wind speed at rated (approximately 14 m/s) or above (cf. Figure 2.4), such that the generator must be controlled to operate at rated power. This is done by regulating the generator to operate at constant rotor speed and constant torque, and hence at constant power. Such regulation is obtained by pitching the blades[4] so as to adjust the aerodynamic torque at each mean wind speed value [21] up to the cut-off speed at approximately 25 m/s. Since almost all turbines today of reasonable size are equipped with pitchable blades, is this the control input variable in Region III that will be investigated in the following. The WT operation in the three regions will yield a *power curve* similar to what is shown in Figure 2.4.

2.5 Components of a WT

The WT is a system composed of many different parts. The most important ones will be described briefly having Figure 2.5 as background.

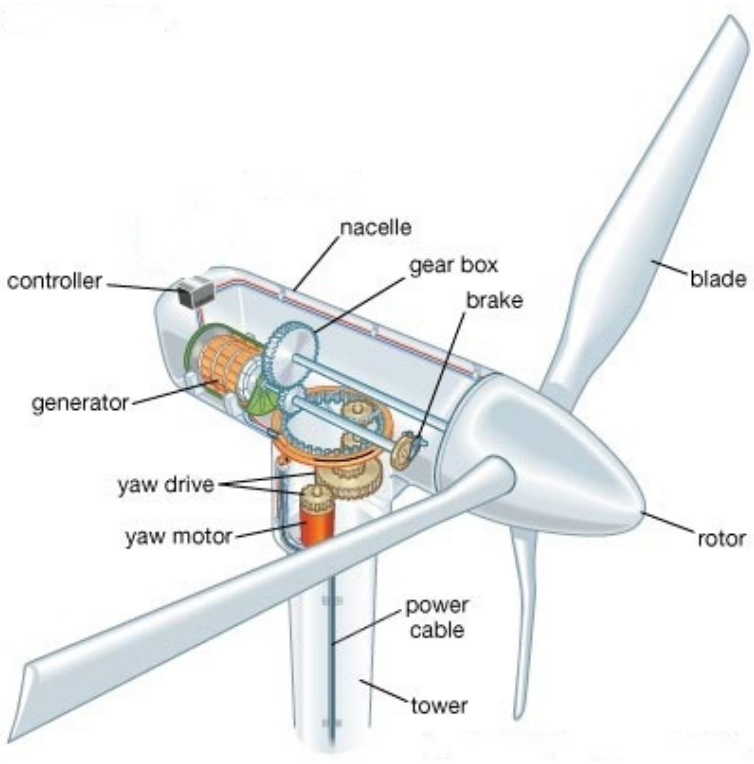

Figure 2.5: Components of a regular WT according to the Danish concept [16]

The WT Rotor

[4]Another method of regulating the torque is by yawing the turbine out of the wind, but this control scheme is now out-of date and will not be covered in this project

The rotor is the part of the turbine that consists of both the turbine hub and the blades. The function of the blades is, as has already been described, to capture the highest amount of energy from the wind. The purpose of the hub is to connect the pitch servos (not shown in Figure 2.5) that adjust the blade direction to the low-speed shaft.

Much effort has been laid down among WT manufacturers to increase the efficiency of the rotor and hence the maximum energy capture of the machine [3], both when it comes to blade shape and also with regard to material selection. However, lighter and more flexible components often result in more flexible structures, which increases the danger of fatigue. It is here that WT control comes in as an important factor, especially independent blade pitch control, which has shown to have a good effect when appropriately designed and adjusted to the specific application [12].

The reason why present WT configurations have three blades rather than two is mainly to reduce the rotational speed, which makes them less disturbing in the landscape and less radiant when it comes to noise [1]. A two bladed rotor also suffers from more load fluctuations due to the fact that the uppermost blade experience the highest wind at the same time as the lowermost passes the tower.

The size of the rotor on modern wind turbines are quite amazing. A typical 5 MW turbine, a common turbine size [50] nowadays have a rotor blade diameter of 126 meters and is sweeping an area of over 12,000m^2.

Drive Train

The drive train consists of the main bearing, the high-speed shaft connecting the gearbox to the generator, a 2- or 3-stage speed-increasing gearbox, and low-speed shaft connecting the rotor to the gearbox.

Generator

Generators are typically asynchronous operate at 550-690 V (AC). The size of the generator is dependent on the blade properties, since this is what directly determines how much torque, and hence power the turbine can generate.

Pitch and Yaw Mechanisms

The pitch angle is the angle at which the blade surface contacts the wind. It is desirable to be able to adjust this angle to ensure optimum operation of the turbine in varying wind conditions and to prevent electrical overload and over speed in high winds. The pitch actuators is therefore an integrated part of the load control system.

The yaw angle is the orientation of the nacelle in relation to the wind. Hence the yaw mechanism, which consists of an arrangement for turning the nacelle, can in the same as with the pitch mechanism be used to actively control the load. Nowadays, when having the pitch mechanism is such control not needed, and the function of the yaw control is to direct the rotor against the wind.

2.6 Fatigue in WTs

The aerodynamic effects from the wind can in general be divided into three the following three main categories of loads

1. Steady state aerodynamic forces generated by the mean wind speed

2. Periodic aerodynamic forces generated by effects as wind shear, rotor rotation, and tower shadow

3. Fluctuating forces induced by wind gusts and turbulence

The second and third category are of special interest when the matter of fatigue is concerned. The periodic forces due to wind shear, yaw misalignment (i.e the nazelle is not directed into the wind appropriately) and/or the stochastic nature of turbulence act together to produce asymmetric loading across the WT rotor. These loads will produce bending moments in the blades which in turn will reach to the main shaft through the hub connection, and may cause the shaft to be radially displaced. This effect can be accounted for by use of a control system, for instance through the blade pitch system. This will reduce the fatigue loading on various turbine components.

Hence, WTs are subjected to a very complex system of variable loads, and can be regarded as being fatigue critical machines [56]. This means that the design of many of the WT components is dictated by fatigue considerations. Although lifetime of a WT is expected to be at least 20 years [32], fatigue damage accumulation has shown to significantly reduce this lifetime. As an example, the result of not accounting for turbulence induced loads in the early days of the multi-megawatt machines in the beginning of 1980s was break-down after months in operation. Hence, the ability to predict wind loads that contribute to fatigue became a critical task in the design of WTs. As WTs with larger diameters are placed on taller towers, fatigue loads become the governing loads for blade design [32].

Among the first to thoroughly cover the issue of fatigue and develop fatigue analysis tools for WT systems are Sandia Laboratory in US. A report from 1999 [56] were written with the background that WT components (primarily blades and blade joints) were seen to fail at unexpectedly high rates. The aim of the report was to give WT designers a way to analyze the fatigue behavior of WT components such that prediction of service lifetime could become an essential part of the design process.

In spite of its actuality are details on the fatigue problem not to be covered in this work. However, the fatigue problem is still implicitly taken into account since the control system in this work will aim at load attenuation through speed regulation.

Chapter 3

Modeling of the Wind Turbine

3.1 Introduction

There are different methods available for modeling purposes. Large multi-body dynamics codes, as reported in [25], divide the structure into numerous rigid body masses and connect these parts with springs and dampers. This approach leads to dynamic models with hundreds or thousands of DOFs. Hence, the order of these models must be greatly reduced to make them practical for control design [61]. Another approach is an assumed modes method. This method discretize the WT structure such that the most important turbine dynamics can be modeled with just a few degrees of freedom. Designing controllers based on these models is much simpler, and captures the most important turbine dynamics, leading to a stable closed-loop system [61]. The method is for instance used in FAST, a popular simulation program for design and simulation of control system [47].

Then, how complex should the model in our case be? If it is too simple, important dynamics will be excluded, which most likely will lead to an unstable closed-loop system or a control algorithm that does not perform as intended. On the other hand, a very complex model will lead to a control system that is too complicated and difficult to design, implement, test, and debug. Under any conditions, however, should the simplified model used for control design depend directly on the control objectives that are identified.

This chapter will present a simplified control-oriented model. In this approach, a state space representation of the dynamic system is derived from of a quite simple mechanical description of the WT. This dynamic state space model is totally non-linear due to the aerodynamics involved, and will thus be linearized around a specific operation point. As reported in [61] with corresponding references, good results are obtained by using linearized time invariant models for the control design.

When modeling a WT one may need to combine different models, each representing interacting subsystems, as Figure 3.1 below depicts. Here we can see how the WT is simplified to consist of the aerodynamic-, mechanical- (drive train), and electric subsystem, and that the blade pitch angle reference and the power reference in this case are controllable inputs.

The WT is a complicated mechanical system with many interconnecting DOF. However, some of the couplings are rather weak and can be neglected [24]. For instance, the connection between the dynamics of the transmission and the tower is neglected in modeling of the mechanical system. The dynamics of the generator

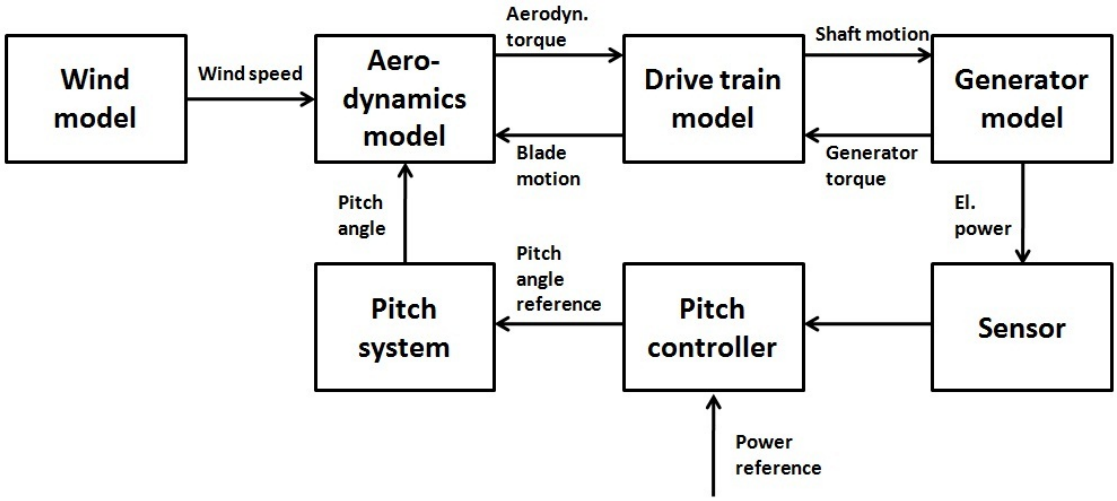

Figure 3.1: WT subsystems with corresponding models

and the electrical system are also neglected by regarding the reaction torque from the generator as a fixed value. Also when considering the wind, the approach is to model the wind as simply a scalar input affecting the rotor state.

The aerodynamic model (cf. Figure 3.1) was presented in Chapter 2. A simplified dynamic model of the mechanical subsystem (i.e the drive train) is presented in this chapter. This model will be used for the control design in Chapter 4 and 5.

3.2 Control Design Steps

As was described in Chapter 3 is it important that the control system must be designed to take into account the most important aero- and structural dynamic properties of the different subsystems, as well as the coupling between them. This means that after the control objectives have been precisely described, the control design must rest upon an appropriate, but of course simplified, dynamic model of the system. This model must then be linearized around a specified operating point (in our case for an above rated wind speed).

The next step in the controller design process should be to perform dynamic non-linear simulations with the controller in the loop to test closed-loop system performance [1]. At this point the control designer may be needed to update the objectives and/or do adjust the model. Following this is the final and very important part of implementing the control algorithms in controller software for field testing on a real turbine. In our case is the practical implementation omitted (no real turbine is available!)

3.3 Establish Control Objectives

It is important to have the objectives of the controller in mind when working with the control design. These objectives depends directly on the turbine configuration. As has already been mentioned is the so-called Danish design (see Section 2.4) regarded as the only turbine configuration covered in this work. Hence, rotor

[1] Since a non-linear simulation model has not been available for this project are the simulations restricted to the Linear Time Invariant (LTI) case

collective pitch will be applied to regulate turbine speed in Region III. Another necessary objective is to maintain stable closed-loop behavior for the given wind disturbance.

3.4 State Space Representation

The nonlinearities of a WT system, for instance due to the aerodynamics, may bring along challenges when it comes to the control design. Since the control input gains of a pitch control usually is the partial derivative of the rotor aerodynamic torque with respect to blade pitch angle variations, these input gains will depend on the operating condition, described by a specific wind and rotor speed. A controller designed for a turbine at one operating point may give poor results at other operating conditions. In fact, a controller which has shown to stabilize the plant for a limited range of operation points, may cause unstable closed-loop behavior in other conditions.

A method which bypasses the challenges of directly involving the nonlinear equations is by using a linear time invariant system (LTI) on state space form. Such a system relates the control input vector u and output of the plant y using first-order vector ordinary differential equation on the form

$$\begin{aligned} \dot{x} &= Ax + Bu + \Gamma u_D \\ y &= Cx + Du \end{aligned} \tag{3.1}$$

where x is the system states and matrices A, B, Γ, C and D are the state-, input-, disturbance-, output- and feedthrough- matrix, respectively, and u_D is the disturbance input vector.

The representation of the system as given in Eqns. (3.1) has many advantages. Firstly, it allow the control designer to study more general models (i.e., not just linear or stationary ODEs). Having the ODEs in state variable form gives a compact, standard form for the control design. State space systems also contain a description of the internal states of the system along with the input-output relationship. This helps the control designer to keep track of all the modes (which is important to do since a system can be internally unstable, although it is input-output stable). As shall be shown in the following is a description of the dynamics on state-space a good starting point for the further controller and observer designs.

3.5 Control Oriented Dynamic Model

The WT drive-train modeled with its high and low speed shaft separated by a gearbox is shown in Figure 3.2. As can be seen from this figure, is the drive train modeled as a simple spring-damper configuration with the constants K_r and C_r denoting the spring stiffness and damping in the rotor shaft, and similarly; K_g and C_g as representing the spring stiffness and damping in the generator shaft. Figure 3.2 also shows the inertia, torque, rot. speed and displacement of the rotor and generator shafts. The parameters named as T1, ω_1, q1, N1,I1 are the torque, speed, displacement, number of teeth, and inertia of gear 1, and similarly for gear 2.

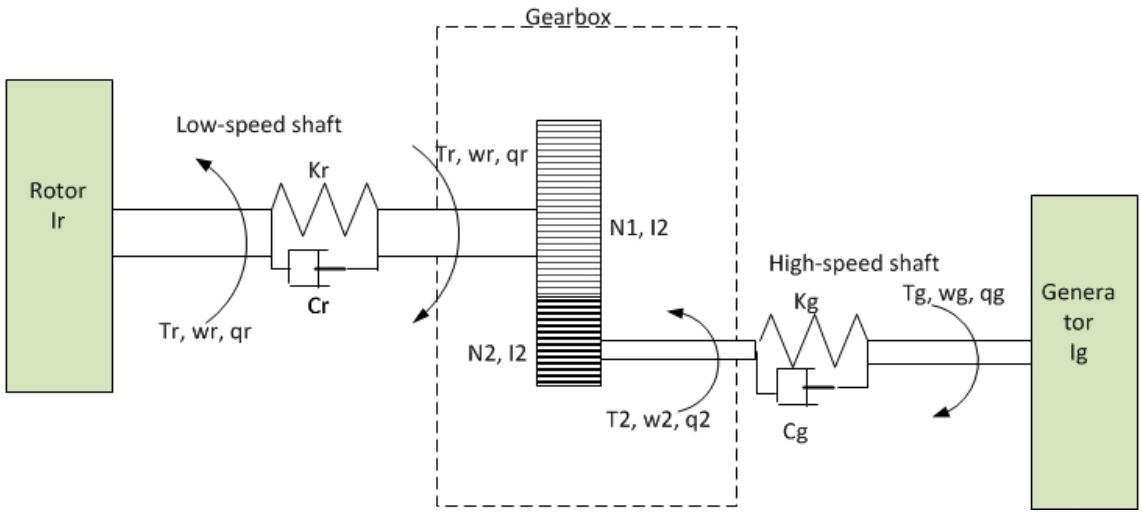

Figure 3.2: Model of the drive train with the high and low speed shafts. (For definition of the parameters, see text)

The model in Figure 3.2 results in the following equation of motion for the rotor torque

$$T_r = I_r\ddot{q}_r + K_r(q_r - q_1) + C_r(\dot{q}_r - \dot{q}_1) + T_1 + I_1\ddot{q}_1 \tag{3.2}$$

where the factor $K_r(q_r - q_1) + C_r(\dot{q}_r - \dot{q}_1)$ is the reaction torque in the low speed shaft. Equivalently, the equation for generator motion is as follows

$$T_g = I_g\ddot{q}_g + K_g(q_g - q_2) + C_g(\dot{q}_g - \dot{q}_2) + T_2 + I_2\ddot{q}_2 \tag{3.3}$$

where the factor $K_g(q_g - q_2) + C_g(\dot{q}_g - \dot{q}_2)$ now is the reaction torque at the high speed shaft.

The relationship between T_1 and T_2 is derived based on the equation describing a constrained motion between two gears in the following way

$$\frac{T_2}{T_1} = \frac{\omega_1}{\omega_2} \rightarrow T_1 = \frac{\omega_1}{\omega_2}T_2 \tag{3.4}$$

If this expression for T_1 is substituted into Eqn. (3.11) and having T_2 from Eqn. (3.3) to be

$$T_2 = T_g - I_g\ddot{q}_g - K_r(q_g - q_2) - C_r(\dot{q}_g - \dot{q}_2) - I_2\ddot{q}_2 \tag{3.5}$$

the following equation for the rotor rotation is valid

$$T_r = I_r\ddot{q}_r + K_r(q_r - q_1) + C_r(\dot{q}_r - \dot{q}_1) + \frac{\omega_1}{\omega_2}(T_g - I_g\ddot{q}_g - K_r(q_g - q_2) - C_r(\dot{q}_g - \dot{q}_2) - I_2\ddot{q}_2) + I_1\ddot{q}_1 \tag{3.6}$$

Since the goal of the modeling is to use it for control design, this equation will be simplified in the following.

First, it can be assumed that the the high speed shaft is stiff. This will imply that $T_g = T_2$, $\omega_g = \omega_2$ and so on. Secondly, the gearbox can be assumed lossless, hence the terms involving I_1 and I_2 can be omitted. This reduces 3.6 to

$$T_r = I_r\ddot{q}_r + K_r(q_r - q_1) + C_r(\dot{q}_r - \dot{q}_1) + \frac{\omega_1}{\omega_2}(T_g - I_g\ddot{q}_g) \tag{3.7}$$

The model is now of three degrees of freedom (DOF); rotor speed, generator speed, and a DOF describing the torsional spring stiffness of the drive train. These DOFs correspond with the three states shown in Figure 3.3

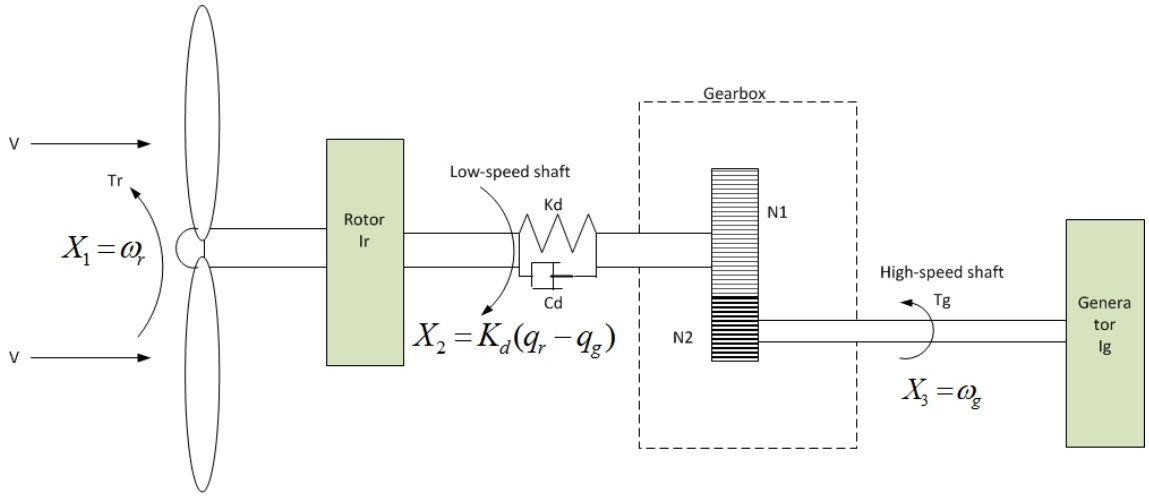

Figure 3.3: Illustration of the 3-state model used in the control design having K_d and C_d as drive train torsional stiffness and damping constants, respectively

The states in Figure 3.3 will in the following be regarded as *perturbations* from an steady-state equilibrium point (operating point), around which the linearization is done. Hence the states are assigned with the δ notation and describes the following DOFs

$$\begin{aligned} X_1 &= \delta\omega_r \text{is the perturbed rotor speed} \\ X_2 &= K_d(\delta q_r - \delta q_g) \text{is the perturbed drive train torsional spring stiffness} \\ X_3 &= \delta\omega_g \text{is the perturbed generator speed} \end{aligned}$$

where $\delta\dot{q}_r = \delta\omega_r$ and $\delta\dot{q}_g = \delta\omega_g$.

Now, from Newtons second law, the following relation is valid

$$I_r\ddot{q}_r = T_r - T_{sh} \tag{3.8}$$

where the left hand side expresses the difference between the aerodynamic torque on the rotor caused by the wind force, and the reaction torque in the shaft. This reaction torque can be expressed according to Eqn.

(3.7) as

$$T_{sh} = K_d(q_r - q_g) + C_d(\dot{q}_r - \dot{q}_g) = K_d(q_r - q_g) + C_d(X_1 - X_3) + \frac{\omega_1}{\omega_2}(T_g - I_g\ddot{q}_g) \tag{3.9}$$

This equation can, when expressed in terms of deviations from the steady state operation point, be written as:

$$\delta T_{sh} = K_d(\delta q_r - \delta q_g) + C_d(\delta\dot{q}_r - \delta\dot{q}_g) + \frac{\omega_1}{\omega_2}(T_g - I_g\delta\ddot{q}_g) \tag{3.10}$$

Recalling from Section 2.3.3, how the torque gained by the rotor from the approaching wind is dependent on the geometric properties of the rotor. Hence the BEM theory provides a way to calculate the power coefficient C_P based on the combination of a momentum balance and a empirical study of how the lift and drag coefficients depend on the the collective pitch angle, β, and tip speed ratio, λ (cf. Section 2.3.2 in Chapter 2). In this way an expression of the aerodynamic torque can be found to be

$$T_r(V, \omega_r, \beta) = \frac{1}{2}\frac{\pi\rho R^2 C_P(\beta, \lambda)}{\lambda}V^2 \tag{3.11}$$

where ρ is the air density, R is the rotor radius, and V is the wind speed.

Let us now assume an operating point at $(V_0, \omega_{r,0}, \beta_0)$ such that Eqn. (3.11) can be written as

$$T_r = T_r(V_0, \omega_{r,0}, \beta_0) + \delta T_r \tag{3.12}$$

where δT_r is deviations in the torque from the equilibrium point ($\delta T_r = T_r - T_{r,0}$) and consists of partial derivatives of the torque with respect to the different variables, i.e Taylor series expansion [35] and [60], in the following way

$$\delta T_r = \frac{\partial T_r}{\partial V}\delta V + \frac{\partial T_r}{\partial \omega_r}\delta\omega_r + \frac{\partial T_r}{\partial \beta}\delta\beta \tag{3.13}$$

where $\delta V = V - V_0$, $\delta\omega = \omega_r - \omega_{r,0}$, and $\delta\beta = \beta - \beta_0$. By assigning α, γ, and ζ to denote the partial derivatives of the torque at the chosen operating point $(V_0, \omega_{rot,0}, \beta_0)$, Eqn. (3.12) becomes

$$T_r = T_r(V_0, \omega_{r,0}, \beta_0) + \alpha(\delta V) + \gamma(\delta\omega_r) + \zeta(\delta\beta) \tag{3.14}$$

If the above expression is put into Eqn.(3.8), it follows that

$$I_r\ddot{q}_r = T_r(V_0, \omega_{r,0}, \beta_0) + \delta T_r - T_{sh,0} - \delta T_{sh} \tag{3.15}$$

At the operation point is $T_r(V_0, \omega_{r,0}, \beta_0) = T_{sh,0}$ since this is a steady state situation. This reduces Eqn. (3.15) to

$$I_r\ddot{q}_r = \alpha(\delta V) + \gamma(X_1) + \zeta(\delta\beta) - X_2 - C_d(X_1 - X_3) \tag{3.16}$$

when substituting with the corresponding state equations. The following expressions for the derivatives of the state variables can now be set up

$$\dot{X}_1 = \frac{(\gamma - C_d)X_1 - X_2 + C_d X_3 + \gamma(\delta\beta) + \alpha(\delta\omega_r)}{I_r} \tag{3.17}$$

$$\dot{X}_2 = K_d(\delta\dot{q}_r - \delta\dot{q}_g) = K_d X_1 - K_d X_3 \tag{3.18}$$

$$\dot{X}_3 = \frac{C_d X_1 + X_2 - C_d X_3}{I_g} \tag{3.19}$$

(Note that in the derivative of the generator speed state X_3 is it used that $I_g\ddot{q}_g = I_g X_3 = \delta T_{sh} - \delta T_g = \delta T_{sh}$ when assuming a constant generator torque).

The dynamic system can now be represented in a state space system on the form as described by Eqns (3.1) yielding

$$\begin{aligned} \begin{bmatrix} \dot{X}_1 \\ \dot{X}_2 \\ \dot{X}_3 \end{bmatrix} &= \begin{bmatrix} \frac{\gamma - C_d}{I_r} & -\frac{1}{I_r} & \frac{C_d}{I_r} \\ K_d & 0 & -K_d \\ \frac{C_d}{I_g} & \frac{1}{I_g} & -\frac{C_d}{I_g} \end{bmatrix} \begin{bmatrix} X_1 \\ X_2 \\ X_3 \end{bmatrix} + \begin{bmatrix} \frac{\zeta}{I_r} \\ 0 \\ 0 \end{bmatrix} \delta\beta + \begin{bmatrix} \frac{\alpha}{I_r} \\ 0 \\ 0 \end{bmatrix} \delta V \\ y &= \begin{bmatrix} 0 & 0 & 1 \end{bmatrix} \begin{bmatrix} X_1 \\ X_2 \\ X_3 \end{bmatrix} \end{aligned} \tag{3.20}$$

where the disturbance input vector u_D from the general form in Eqns. (3.1) now is given as δV, which is the perturbed wind disturbance (i.e deviations from the operating point, $\delta V = V - V_0$), and the control input vector u from Eqns. (3.1) now given as $\delta\beta$ (i.e perturbed (collective) pitch angle, $\delta\beta = \beta - \beta_0$).

The parameters will be assigned when coming to Chapter 5. It is worth no notice that the the measured output signal here is the generator speed. This can be seen from the form of the output vector C. It will be shown later that this will lead to a non-minimum phase plant, i.e a plant with an asymptotically unstable zero in the right complex plane [42]. Such plant is in general not suitable for the LTR approach such that a revision of this is required.

Chapter 4

Wind Turbine Control

4.1 Introduction

In order to have a power production which ensures that speed, torque and power are within acceptable limits for the different wind speed regions, is it necessary to control the WT. This control system should be complex enough to meet the intended control objectives, but at the same time simple enough to easy interpret the results. A frequently used approach, which will also be applied in this work, is to start with a simple model and a simple controller that can be developed further by adding more degrees of freedom into the model.

Optimally speaking, if the control system shall be able to meet the requirement of reduced energy cost, it must find a good balance between (a) a long working life without failures and (b) an efficient (optimal power output) and stable energy conversion. The first point can be regarded as the main focus in this work[1]. This requirement can be further crystallized to the following properties which the control system should possess

- good closed loop performance in terms of stability, disturbance attenuation, and reference tracking, at an acceptable level of control effort.
- low dynamic order (because of hardware constraints)
- good robustness

To meet the objective of long working life should the control system be designed to be efficiently mitigate loads in order to reduce the fatigue stresses (especially in shaft and blade rotor) due to varying wind disturbances. Before going into the specific control design, an historical overview of WT control with a special view toward the objective of load reduction, will be presented in the following.

4.2 History of WT Control

The history of WT control and research within this field have emerged from the simplest form of passive stall control to advanced controllers, like so-called smart rotor control. The latter is well described in for instance [59] and [40]. As these references portrays does this control scheme involve active aerodynamic flow control

[1] Both of these points are important from an economical perspective, but a trade-off between these two will not be discussed in this report.

by implementation of numerous sensors and actuators, bringing along a high level of complexity. Although these advanced control methods have been investigated for ten to fifteen years, most commercial systems are still implemented using multiple single-input-single-output (SISO) loops with classical PID controllers [10]. Actually, as reported in [12], PID showed to give competitive results compared to some of the new advanced techniques.

The traditional way of controlling a WT with multiple control objectives, such as speed control for maximum power tracking and load mitigation by pitch control, is to design independent control loops in a way illustrated in Figure 4.1(a).

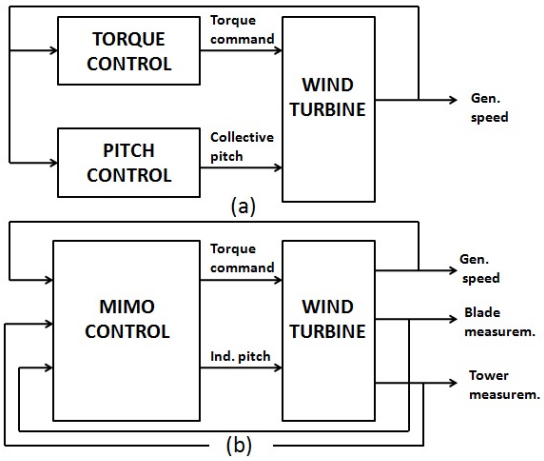

Figure 4.1: Illustration of difference between SISO and MIMO controllers

The PID controllers (i.e. the SISO controllers shown in Figure 4.1 (a)) are traditionally used for the individual torque and pitch control and have shown to have a good effect when carefully tuned and adjusted to its specific application. One disadvantage is, however, that the PID control loops must be designed not to interfere with each other. If this happen to be the case will the result often be a destabilized turbine. This problem can be solved in an efficient manner within the modern and so-called advanced control techniques [61] using MIMO controllers (cf. Figure 4.1 (b)). In these more advanced control designs, multiple control objectives is seen to be met with fewer control loops leading to stable closed loop behavior [62].

With increasing turbine sizes, much research is done to find new and better ways of load control compared to the classical methods (see [62] and [11] with references). Large turbine sizes will give rise to loads that vary along the blade and change quickly due to wind gusts and other varying wind conditions. Rapidly changing loads can cause fatigue damage and reduce the life of the WT, which in turn may decide the lifetime of the other turbine components. Because of the inertia of the system, as well as the limitations of the actuators, active pitch control alone can only control "average" loads on the blade. On the other hand, passive load control strategies cannot respond to local load variations. Active aerodynamic load control (AALC) is therefore suggested to have a good potential as an addition the existing control strategies when it comes to load reduction [26]. One approach where AALC has been combined with an individual blade pitch control scheme has shown to reduce the root flap bending moment significantly [27].

A well known MIMO controller, the Linear Quadratic Gaussian (LQG) regulator is suggested in [54] to be used in load control. This report present that this regulation policy can have a good load reduction capability for a large frequency range. Reports as [11] and [12] suggest load mitigation when using individual pitch actuators. A thorough study has been performed by Bossanyi in [11] where the classical PI control is

compared with a multi-variable LQG control approach. Although this work has shown to yield good results when applying LQG, the design process is not straightforward and the resulting algorithm is relatively difficult.

One of the disadvantages of LQG design, however, is that it cannot directly take into account robustness margins (like the gain- and the phase margin). Due to this poor robustness properties of LQG control it was been necessary to search after other methods which could handle model uncertainties in a better way. One method which can be traced back to the early 1980s is the H_∞ approach. In this approach does the control designer from the very beginning specify a model of system uncertainties, which can be for instance additive perturbations or output disturbance [22]. Connor, Iyer et.al. [19] were in 1992 among the first to suggest an application of H_∞ control on a WT model. Their main concern in this work were how to reduce the matter of fatigue loading. Although they encountered some overshoot problems did they prove that the method was applicable to a WT control problem. Suggestions of how H_∞ control can be used for load reduction has later been reported in [9]. The method has also been shown to be applicable in advanced power control to enhance a better power capture for a wider range of wind speeds [45].

One particular problem the WT control designers must be able to handle is that WT control generally involves a multi-objective optimization problem, each objective having different goals. For instance, the control objective can be alleviate loads due to large scale gusts over the whole disk area, while others can be more slowly varying and low frequency loads over only one blade. To handle this problem does [15] propose an approach based on a multi-layer architecture. In this method are three control layers designed, each aiming at a specific control target and cooperates with the other layers to obtain various control goals. In this way, the choice of the controller used on each layer can be optimized and tailored to the specific control goal of that layer, thereby improving performance and simplify tuning [15].

What the control designer in all of the above mentioned controlling methods are actually trying to do is to compensate for the stochastic fluctuations in the wind. To do this in a perfect way is of course more or less impossible. One method called Disturbance Accommodating Control (DAC) take into account the fluctuations in the wind by an estimation of the disturbance for an assumed above-rated wind speed situation[2][8]. DAC has shown to have a good effect on load mitigation and is therefore used to obtain special attention when it comes to fatigue load reduction [51]. The theory was thoroughly compared with PI control by Alan Wright in his PhD thesis from 2004 [60]. He concluded in his report that the analytic results obtained using DAC appeared to be "extremely promising". For instance, it was shown how DAC has much better performance compared to the PI control in reducing drive-train shaft torsional moments and blade root flapwise-bending moments [60]. A brief description of the theory behind the DAC will be given shortly, while an implementation and testing of DAC for the WT system will be done in Chapter 5.

In addition to the above mentioned control schemes are methods as Model Predictive Control (MPC) [35], Generalized Predictive Controller (GPC), and Fuzzy Logic Control [39] proposed for WT control. A comparison of different control techniques will not be done in this work (please refer to [13] for more on this).

Since the approach in this work is firstly to apply the DAC approach with LQR regulation. Hence, the first control method which will be described in the following is the LQR. (The actual LQR design to be used in the DAC approach will be described in Chapter 5.) Following this is state estimation covered since no WT system will in practice meet the assumptions a LQR is based upon. Then is the DAC method described briefly and put it into context with LQR and state estimation. The next is then to describe how a LQG

[2] As reported in [61] is the method called Disturbance Tracking Control (DTS) when applied as optimum power point tracking in Region II

regulation procedure can be used in WT control, and further; how LQG can be improved with robust control techniques.

4.3 The Linear Quadratic Regulator (LQR)

The LQR controller was among the first of the so-called advanced control techniques used in control of wind turbines. Liebst presented in 1985 a pitch control system for the KaMeWa wind turbine using LQR design [60]. The objective of this controller was to alleviate blade loads due to wind shear, gravity, and tower deflection using individual blade pitch control. Results of this work included a reduction of blade and tower cyclic responses as well as the reduction of a large 2-per-revolution variation in power [17].

The practical application of this technique is limited by the challenges of obtaining accurate measurements of the states needed in the controller. One way to solve this is to add extra sensors and measurement arrangements. However, since this extra sensors and measurements will add considerable cost and complexity to a WT, is this most often not regarded as a good solution. In addition, errors in the measurement of these states can result in poor controller behavior [60]. To avoid these problems, a state estimator is added in any practical LQR implementation [41]. This approach was described by Mattson in his Ph.D thesis as early as in 1984, where power-regulation for a fixed-speed WT using blade pitch is presented [53]. The proposed solution to the WT control problem was here based on linear models containing drive-train torsion and tower fore-aft bending DOF. The same report also describes the use of state estimation to estimate wind speed.

The principles of a LQR controller is given in Figure 4.2. Here the state space system is represented with its matrices A, B, and C, together with the LQR controller (shown with the $-K$).

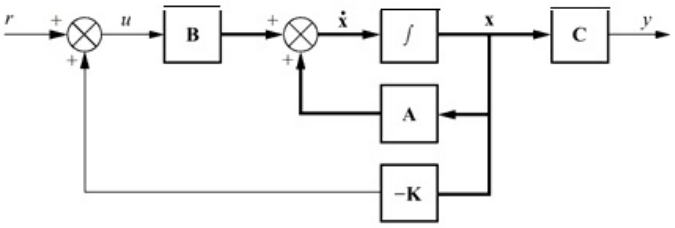

Figure 4.2: State space control using a LQR controller where K is the LQR gain matrix

The LQR problem rests upon the following three assumptions [7]:

1. All the states are available for feedback, i.e it can be measured by sensors etc.
2. The system are *stabilizable* which means that all of its unstable modes are controllable
3. The system are *detectable* having all its unstable modes observable

LQR design is a part of what in the control area is called *optimal control*. This regulator provides an *optimal control law* for a linear system with quadratic performance index yielding a cost function on the form [18]

$$J = \int_0^\infty x^T(t)Qx(t) + u^T(t)Ru(t)\,dt \tag{4.1}$$

where $Q = Q^T$ and $R = R^T$ are weighting parameters that penalize the states and the control effort, respectively. These matrices are therefore controller tuning parameters.

It is crucial that Q must be chosen in accordance to the emphasize we want to give the response of certain states, or in other words; how we will penalize the states. Likewise, the chosen value(s) of R will penalize the control effort u. As an example, if Q is increased while keeping R at the same value, the settling time will be reduced as the states approach zero at a faster rate. This means that more importance is being placed on keeping the states small at the expense of increased control effort. On the other side, if R is very large relative to Q, the control energy is penalized very heavily. Hence, in an optimal control problem the control system seeks to maximize the return from the system with *minimum cost*.

In a LQR design, because of the quadratic performance index of the cost function, the system has a mathematical solution that yields an *optimal control law* given as

$$u(t) = -Kx(t) \tag{4.2}$$

where u is the control input and K is the state feedback gain matrix given as $K = R^{-1}B^TS$. It can be shown (see [18])that S can be found by solving the following algebraic Riccati Equation (ARE)

$$SA + A^TS + Q - SBR^{-1}B^TS = 0 \tag{4.3}$$

The process of minimizing the cost function by solving this equation can easily be done using the built-in MATLAB function `lqr`.

As can be seen from the above description does the LQR algorithm take care of the tedious work of optimizing the controller, which for the case of the PID controller can be a time consuming task. However, the control designer still needs to specify the weighting factors and compare the results with the specified design goals. This means that controller synthesis will often tend to be an iterative process where the designed "optimal" controllers are tested through simulations and will be adjusted according to the specified design goals.

The optimal control solution from the LQR approach yields some impressive properties. Firstly the controller guarantees at least 60° phase margin in each input channel [52], which means that as much as 60° phase changes can be tolerated in each input channel without violating the stability. In addition, the LQR has infinite gain margin which implies that the LQR is still able to guarantee the stability, even though the gain increases indefinitely. Hence, LQR guarantees a very robust controller, capable of handling various kinds of uncertainties in the modeling. However, when an state estimator is implemented with measurement feedback, these properties just described is often lacking. But, as will be shown later; the robustness properties can be recovered!

4.4 State Estimation

As mentioned for the case of the LQR controller, all sensors for measuring the different states are in this case assumed to be available. This is not a valid assumption in practice. A void of sensors means that all states (full-order state observers), or some of the states (reduced order observer), are not immediately available for use in the control task. In such cases, a state observer must be implemented to supply accurate estimations

of the states at all wind-rotor positions. The schematics of the system with the observer is shown in figure 4.3 below.

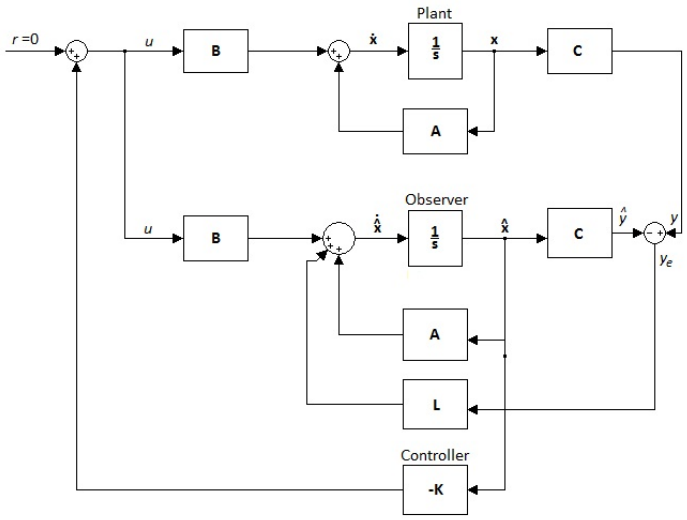

Figure 4.3: Schematic of state space control using a observer where L is the observer gain and K is the LQR gain matrix

As can be seen from figure 4.3, the observer state equations are given by

$$\dot{\hat{x}} = A\hat{x} + Bu + L(y - C\hat{x}) \tag{4.4}$$

$$\hat{y} = C\hat{x} \tag{4.5}$$

where $\hat{x}$ is the estimate of the actual state x. Furthermore, equations (4.4) and (4.5) can be re-written to become

$$\dot{\hat{x}} = (A - LC)\hat{x} + Bu + Ly \tag{4.6}$$

These are the governing equations for a *full order observer*, having two inputs u and y and one output, $\hat{x}$. Since we already know A, B, and u, observers of this kind is simple in design and provides accurate estimation of all the states around the linearized point. From Figure 4.3 we can see that the observer is implemented by using a duplicate of the linearized system dynamics, with an additional gain on the estimation error. In this way the difference between the measured and the estimated outputs will be fed back to correct the model continuously. The proportional observer gain matrix, L, can be found for instance by pole placement procedure, or as will be shown in the following; by applying the Kalman filter design.

4.4.1 Kalman Estimator

In the previous design of the state observer, the measurements $y = Cx$ were assumed to be noise free. This is not usually the case in practical life. Other unknown inputs yielding the state equations to be on the

general stochastic state space form, which is already defined in Eqn. (3.1) as

$$\dot{x} = Ax + Bu + \Gamma u_D$$
$$y = Cx + Du + n$$

here the D matrix relating the input u to the output y most commonly is set to zero, the disturbance input vector u_D is stationary, zero mean Gaussian white process noise (i.e wind disturbance), and n is zero mean Gaussian white sensor noise.

The Kalman filter can be applied to yield the estimated state vector $\hat{x}$ and output vector $\hat{y}$ (cf. Eqns (4.4) and (4.5), by using the known inputs u and the measurements y. Block schematics of a Kalman filter connected to the plant is depicted in Figure 4.4.

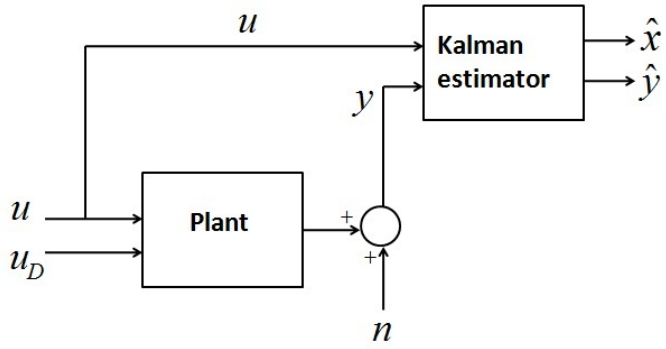

Figure 4.4: Kalman filter used as an optimal observer

It can be shown that this will result in an optimal state estimation. The Kalman filter is optimal in the sense that it minimizes the estimated error covariance when some presumed conditions are met [14]. The mean-square estimation error is given by

$$J = E[(x(t) - \hat{x}(t))^T (x(t) - \hat{x}(t))] \tag{4.7}$$

where

$$E[(x(t) - \hat{x}(t))^T y(t) = 0 \tag{4.8}$$

The optimal Kalman gain is given by

$$L(t) = S_e(t) C^T R^{-1} \tag{4.9}$$

where $S_e(t)$ is the same as J given in (4.4.1). Furthermore, when $t \to \infty$, the algebraic Riccati equation can be written as

$$0 = S_e A^T + A S_e + Q_n - S_e C^T R_n^{-1} C S_e \tag{4.10}$$

where Q_n and R_n are the process and measurement noise covariances, respectively. Tuning of the Kalman filter are required if these are not known. Finally, the sub-optimal Kalman gain for a steady state Kalman

filter can be expressed as $L = S_e C^T R^{-1}$.

4.5 Disturbance Accommodating Control

This section will explain the principles of DAC[3]. The DAC method will be utilized together with a LQR regulator and is a straightforward way to model and simulate a system with an assumed-wind disturbance.

Recalling from the state space system described by Eqns. (3.1), which included the vector Γ. This vector describes the magnitude of the disturbance, while the input signal u_D is the disturbance quantity (which in our case is the wind speed perturbation). The Γ vector will in the DAC procedure be used as a free design parameter.

The basic thought in DAC theory is that disturbances are described by an assumed-waveform model on state space form. Such a wind model can be described according to the following equations [60]

$$\dot{z}_D = F z_D \tag{4.11}$$
$$u_D = \Theta z_D \tag{4.12}$$

where z_D denotes the disturbance state, F the state matrix, u_D is disturbance output vector (input to the plant), and Θ relates disturbance model input to disturbance states. Note that it is necessary to know something about the initial condition of the disturbance state, z_D^0, in order to know the amplitude of the disturbance.

Since the state variables x and the disturbance variable z_D cannot be measured directly, observers will be utilized to estimate these. The mathematical description of the observer will in this case according to Eqns (4.4) and (4.5) be given as

$$\dot{\hat{x}} = A\hat{x} + Bu + \Gamma\hat{u}_D + K_x(y - \hat{y}) \tag{4.13}$$
$$\hat{y} = C\hat{x} \tag{4.14}$$

where the estimator gains K_x can be chosen according to for instance the pole placement method using the `place` command in MATLAB.

Furthermore, the disturbance observer is described as

$$\dot{\hat{z}}_D = F z_D + K_D(y - \hat{y}) \tag{4.15}$$
$$\hat{u}_D = \Theta \hat{z}_D \tag{4.16}$$

where the disturbance state estimator gain K_D is a scalar.

The estimated variables can then be fed into the controller to minimize the effect of the disturbances. The result of this is that the state feedback now also include the feedback of disturbance observer yielding a

[3]For more details, please refer to e.g. [38]

"new" feedback control law on the form

$$u(t) = G\hat{x}(t) + G_D\hat{z}_D(t) \tag{4.17}$$

where the LQR gain G is computed in MATLAB, and the full state feedback gain (i.e disturbance gain) G_D must be chosen as to minimize the norm $|BG_D + \Gamma\Theta|$. Calculated numerical values will be given in Chapter 5.

4.6 The LQG Controller

Another well-known method of handling noise inputs is the Linear Quadratic Gaussian (LQG) controller. This is simply a combination of a Kalman filter and a LQR controller. The separation principle guarantees that these can be designed and computed independently [49]. LQG controllers can be used both in linear time-invariant (LTI) systems as well as in linear time-variant systems. The application to linear time-variant systems enables the design of linear feedback controllers for non-linear uncertain systems, which is the case for the WT system.

The schematics of a LQG is in essence similar to that depicted in Figure 4.3 in Section 4.4, the only difference is that the observer gain matrix L in this figure now can be defined as the Kalman gain K_f. However, we also assume disturbances in form of noise, such that the system with the LQG regulator in compressed form can be described as in Figure 4.5

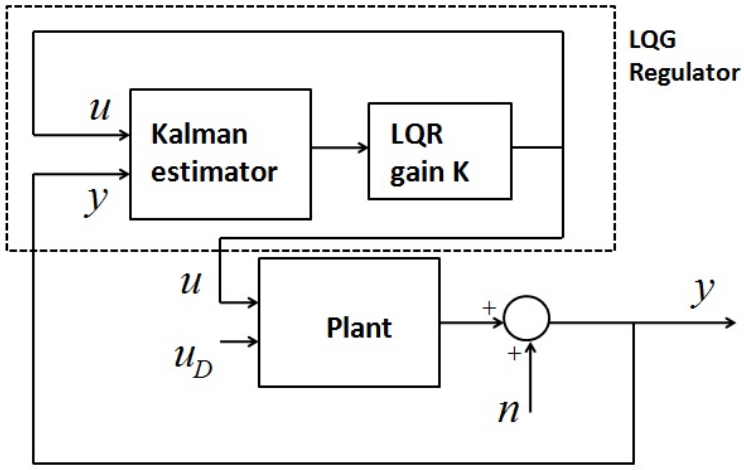

Figure 4.5: LQG regulator

4.7 Robust Control

4.7.1 Introduction

As seen so far, a control system's optimality according to some specified criterion is obtained from a linear quadratic controller. However, optimality cannot be the only desirable property of a controller. When

designing a control system for a feedback system, one usually require the control system to meet certain closed-loop objectives with regard to the *performance*, in addition to the fundamental requirement of merely stabilizing the plant. This performance can be defined in terms of objectives such as the controller's ability to follow a predefined command, the fastness of the response, and disturbance rejection.

One question which arises when implementing a control system in real-life is how capable it is to maintain stability and performance in spite of uncertainties as bounded modeling errors and unpredicted noises. Due to the fact that the model is simplified a lot and the disturbances are not easy to predict in a precise way, it is necessary with some additional work regarding the *robustness* properties.

Robustness is a measure of how sensitive the control system is to unpredicted errors with respect to system dynamics and/or in the working environment. The theories on the field of robust control began in the late 1970s and early 1980s and were soon developed into a number of different techniques for dealing with uncertainties in dynamic systems. For instance, lack of phase information in MIMO systems makes prediction of stability in closed-loop impossible. To handle this problem and perform a robust stabilization of the closed loop system, the H_∞ loop-shaping method was developed [22]. The method augments the plant with appropriate chosen weights so that the frequency response of the open-loop system is shaped to meet the closed loop performance requirements. Another example for improving the robustness, which in many ways can be regarded as a loop-shaping procedure, is the Loop Transfer Recovery (LTR) method. This method was originally developed to overcome robustness problems, i.e lack of phase margins, of observer based controllers like the LQG [52].

4.7.2 Loop Shaping and the LTR Procedure

When the present plant model uncertainty is high, then the use of large feedback gains may cause an unstable system. Plant model uncertainty can therefore be a limiting factor in determining what can be achieved with feedback [28][4].

One of the key ideas behind the concept of loop shaping is to use the same approach as with the *Nyquist Stability Criterion*, where closed loop stability for SISO systems is investigated by studying the open loop transfer function (TF). Hence, loop analysis involves shaping the gain of the open loop TF, $L = G * K$ (cf. Figure 4.6 below). Here does G denote the plant and K the controller, or compensator. Note that the loop in this case is broken at the output port of the plant. This means that the unstructured uncertainties in the model is reflected at this point.

Loop shaping can therefore be regarded as a tool to see the impact in the controller K if the desired performance in terms of the properties of L can be specified. This will say that we have to know something about how K can be adjusted to meet the desired specifications in L. A direct loop-shaping approach will not be considered in this work, but instead a method implementing some of the elements of loop-shaping, the Loop Transfer Recovery (LTR) approach.

The LTR has been a popular model-based frequency domain design method in the industry for decades, for instance among aircraft control system engineers [57]. The systematic design procedure provided by LTR were originally designed as an extension to observer based controllers, such as the LQG regulator [52], and one of the reason for its popularity can therefore be traced back to the intuitive relationships the method gives between full state feedback designs and observer based designs. The LTR method is therefore a way

[4]This project will not go into details on model uncertainty analysis and its impact on the control system, but will only assume uncertainties to be present, requiring a certain robustness of the control system

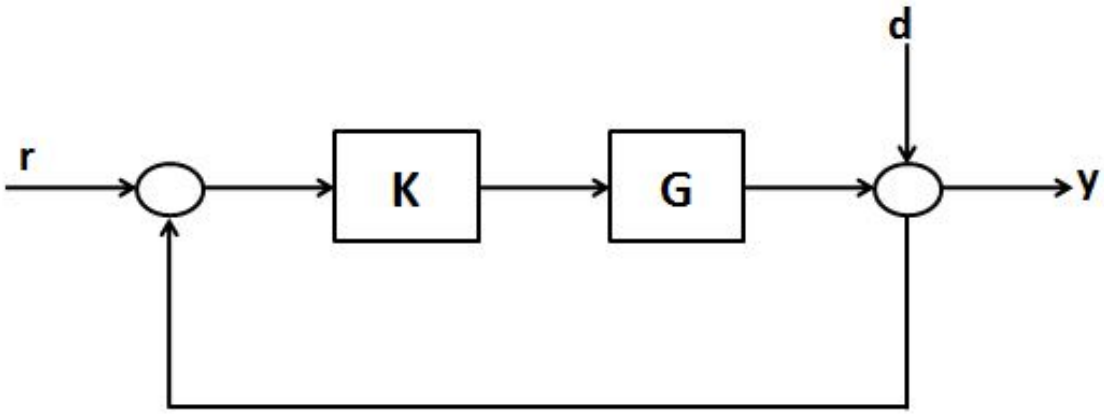

Figure 4.6: Basic feedback loop configuration

to handle a problem often encountered by control designers when implementing an observer-based feedback observer to a full-state feedback system (as LQG); a loss of the gain and phase margins present at an optimal state-feedback. Hence, by applying the procedure of LTR, the aim is now to recover the loop shape, i.e the lost robustness, due to the implementation of an observer. It is important to note that the LQG/LTR procedure works only if the plant is minimum phase, and has at least as many inputs as outputs.

It is when applying the LQG/LTR technique common to use a two-step procedure. The exact design procedure of the LQG/LTR depends on the point where the unstructured uncertainties are modeled. Most commonly is this either the input or the output port of the plant [52]. The following two-step procedure is based on the assumption that the plant uncertainties are reflected at the output port.

The first step is to construct a compensator, or a filter, yielding desired response in accordance with the defined performance specifications. Hence, it is firstly necessary to have a "model" of the plant, called the Target Feedback Loop (TFL), where disturbances are modeled as load and measurement noise, and the compensator gain K_f is designed to attenuate these noises. As has already been described is the Kalman filter an optimal way of compensating for process and measurement noises. Hence, since the underlying idea of the LQG/LTR can be viewed as a way to treat the unstructured uncertainties on the plant as noises [2], a Kalman filter can be applied as a “fictious” filter designed to reject these noises. In this first design step, the TFL with desired loop shape is therefore constructed via Kalman filter. In other words, the Kalman filter is in this step applied to obtain a loop that serves as a target to which the controlled system is to converge.

It is first assumed the system as given in (3.1). After the measurement and disturbance noise covariance matrices are determined, the MATLAB function `kalman` can be used to find the optimal Kalman filter gain L and the covariance matrix P. Measurement noise covariance matrix is determined out from an expected noise on each channel. The transfer function of the Kalman filter composing the TFL will then be given as

$$G_{TFL} = C(sI - A)^{-1}L \tag{4.18}$$

Note that to be able to ensure that the gain matrix L is able to stabilize the TFL, [A,C] must be observable.

Then with reference to the feedback loop in Figure 4.6, one may ask if there exists a compensator K which has the same properties, and can meet the same requirements in the robustness and performance as the TFL just designed does. If so, it is quite obvious that the open loop transfer function $L = G \cdot K$ then have to

approximate G_{TFL} over the frequency range of interest. The second step in LQG/LTR method guarantees this to be true.

The second step is to do an optimal controller design to recover the gain found in the first step, which is done by solving the Riccati equation as in LQR. However, in this case the Riccati Equation will include a correction term, the "LTR gain", given as ρ in the following way

$$SA + A^T S + \rho Q - SBR^{-1}B^T S = 0 \tag{4.19}$$

For the LQG/LTR to guarantee for a recovery of gain, then $\rho \to \infty$ [7]. This yields the control gain matrix

$$K = R^{-1}B^T S \tag{4.20}$$

It can be shown [7] that if the state space system (given as G in Figure 4.6) is of minimum phase, the transfer function $L = G \cdot K \to G_{TFL}$. The "recovered" Kalman filter loop gain results in infinite gain margin and +/- 60°. phase margin in each of the feedback loops. The recovered loop shape can then realized through frequency response methods such as Bode or Nyquist plots. In this work a dynamic compensator extracted from the LTR algorithm will be used to see how the LTR methods can improve the regulation capability of mitigating wind disturbance input.

Chapter 5

Control Design and Simulations

5.1 Introduction

The purpose in this project is to investigate the application of modern control theories, such as the LQR and LQG, on WT systems and how a speed controller can be made with these theories to reduce torque variations due to a wind disturbance. In addition, a further idea is to investigate if a better load reduction can be obtained by using a dynamic compensator from the LTR algorithm, and whether factors as the LTR gain will affect this result.

The simulations are done in the MATLAB Simulink environment, enabling the LTI state space model described in Chapter 3 to be incorporated together with the different controllers in the convenient block diagram approach available in Simulink.

This chapter will present results from the practical implementation of the WT control design. It is important to note that a test of the controlled system under various operating conditions has not been performed. This is mainly due to the fact that this work is not focused on a real-life application of the controller, but instead on the theoretical aspects of controller design. Also, the linearization of the WT plant at different operation points would have required a computer program, such as FAST[1]. Load mitigation in above rated wind speeds has already been described to be the focus of this work, and the operation point chosen will reflect this goal.

The first control approach that is being tested is the DAC theory, where the wind disturbance modeled in a straightforward way together with the LQR and observer procedures, as described in Chapter 4. The reason for starting with this method is to investigate if the results are comparable with the results from the LQG method, and if so; what is the difference in the results, and which results can be regarded as the "best" results.

It is important to note that for the simulations in this project are the actuator constraints, such as the dynamics of the pitch-system, not taken into consideration.

[1] A popular aeroelastic design code for horizontal axis wind turbines developed by National Renewable Energy Laboratory, USA [47]

5.2 Linearization

As was described in Chaper 2 does the WT compose of a complex non-linear relationship between factors such as the aerodynamic properties of the blades, pitch angle, and wind speeds. The best approach is thus to build the model out from experimental data and a non-linear simulation model of the WT. Although it is possible to build a non-linear WT simulation model also in Simulink and extract linear models by utilizing the built-in `trim` and `linmod` functions, has this not been done in this work. Since the mathematical model presented in this report is simplified a lot would this approach probably result in a more inaccurate model than with the use of the tailored WT simulation code provided by FAST, where many aspects regarding the aerodynamics and structural dynamics are taken into account. The linearized state space model, which will be used in the control design is based on what is presented in [60] and [8].

The operation point, around which the linearization is done, is given as [60],

$V_0 = 18m/s$
$\omega_{rot,0} = 42rpm$
$\beta_0 = 12°$

The corresponding FAST linearization with reference to [60] around this point yields the following state space system

$$\begin{bmatrix} \dot{X}_1 \\ \dot{X}_2 \\ \dot{X}_3 \end{bmatrix} = \begin{bmatrix} -0.145 & -3.108 \cdot 10^{-6} & 0.02445 \\ 2.691 \cdot 10^{7} & 0 & -2.691 \cdot 10^{7} \\ 0.1229 & 1.56 \cdot 10^{-5} & -0.1229 \end{bmatrix} \begin{bmatrix} X_1 \\ X_2 \\ X_3 \end{bmatrix} + \begin{bmatrix} -3.456 \\ 0 \\ 0 \end{bmatrix} \delta\beta + \begin{bmatrix} 1 \\ 0 \\ 0 \end{bmatrix} (\delta V) \tag{5.1}$$

$$y = \begin{bmatrix} 0 & 0 & 1 \end{bmatrix} \begin{bmatrix} X_1 \\ X_2 \\ X_3 \end{bmatrix}$$

where the factors C_d/I_{rot} and C_d/I_{gen} are calculated by using the known relation to the other parameters.

Recalling from Chapter 3 that Γ vector is given as $\frac{\alpha}{I_r}$, where α is describes the relationship between torque variations and wind variations, $\frac{\partial T_r}{\partial V}$. This means that if Γ is increased, it will follow that the torque is more sensitive to wind variations, which is surely a negative effect when the matter of fatigue is concerned. The torque is given as a non-linear function in Eqn (3.11), which shows the dependency on the wind speed, rotor speed and blade pitch, and will be fixed at the chosen operating point. However, the Γ vector is initially chosen to $[100]^T$.

The transfer function (TF) of the open loop system formed by the linearized state space system in Eqns. (5.2) is

$$G(s) = \frac{1.499 \cdot 10^{-14} s^2 - 0.4247s - 1450}{s^3 + 0.374s^2 + 503.3s + 59.44} \tag{5.2}$$

extracted by using the MATLAB function `ss2tf`

One of the zeros of this TF is located at $s = 2.83 \cdot 10^{13}$ leading to a non-minimum phase system. Since the LTR procedure applied as an extension to the LQG later on is not feasible for non-minimum phase systems

[52] will this vector be formed as to represent rotor speed measurement instead, which changes the output to

$$y = \begin{bmatrix} 1 & 0 & 0 \end{bmatrix} \begin{bmatrix} X_1 \\ X_2 \\ X_3 \end{bmatrix} \tag{5.3}$$

The plant TF is now

$$G(s) = \frac{-3.456s^2 - 0.7914s - 1450}{s^3 + 0.374s^2 + 503.3s + 59.44} \tag{5.4}$$

having zeros and poles located as shown in Figure 5.1 below.

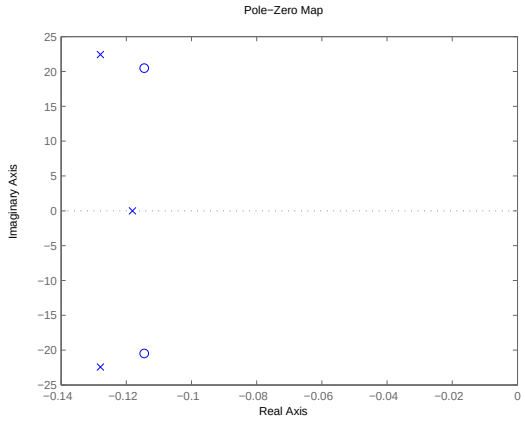

Figure 5.1: Poles (marked with X) and zeros (marked with O) for the plant TF with measured rotor speed

As Figure 5.1 portrays is this plant now of minimum phase (i.e no zeros in right complex plane).

5.3 Disturbance Accommodating Control

The DAC procedure has already been described in Section 4.5. The Simulink block digram shown in Figure 5.2 was set up according to the governing equations described in this section.

The assumed waveform model is shown in Figure 5.2. It is assumed a step input disturbance from the wind, hence $F = 0$ and $\Theta = 1$ will be chosen to reflect this [35]. In order to "excite" the controller an initial condition (chosen as 1) were inserted into the integrator of the disturbance model.

Simulation Without any Control

It is interesting first to have a look at the response without any control at all. Then, after implementing the controller, is it easier to see how good the controller works in the disturbance accommodating task.

Now, by setting both the LQR and the wind disturbance gain equal to zero, perturbations in rotor speed (i.e. deviation from the operation point) shown in Figure 5.3 when simulating for 50 seconds. According to

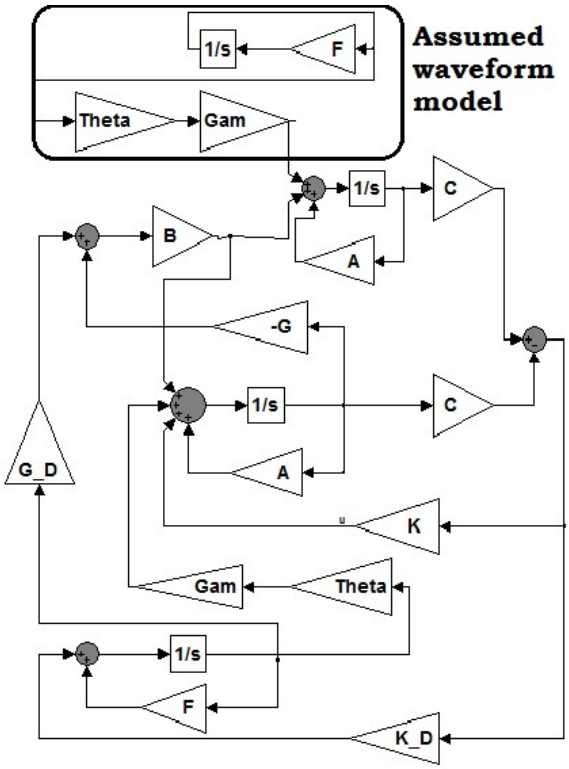

Figure 5.2: Simulink block diagram of DAC

the simulation result, it is observed that the wind disturbance is not accommodated, and the rotor speed will increase.

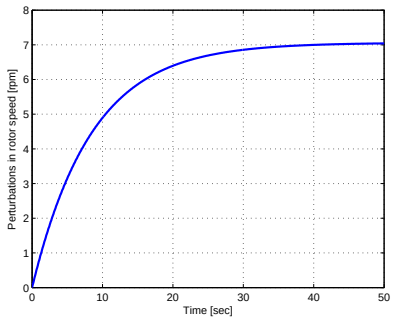

Figure 5.3: Perturbations in rotor speed with no control

Simulation with only Wind Disturbance Gain

The next scenario which is to be simulated is a situation with the LQR control gain set to 0, but with the wind disturbance state gain G_D set to minimize the norm $|BG_D + \Gamma\Theta|$. The response of the rotor speed is shown in Figure 5.4 below.

As can be seen in this plot does G_D alone manage to regulate the speed, but with a long settling time.

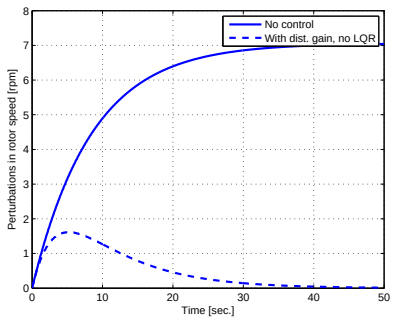

Figure 5.4: Perturbations in rotor speed with disturbance gain

Simulation of DAC with LQR

The final DAC approach will involve a LQR design. Hence, this design will be described in the following, with reference to the theories on LQR presented in Section 4.3. The complete MATLAB code used is given in the Appendix.

One of the first thing to check in the LQR design is whether the state space system is controllable and observable. Using the MATLAB functions `obsv(A,C)` and `ctrb(A,B)`, where A, B, and C are the state-matrices from the linearized states space model, is the observability matrix found to be

$$Ob = \begin{bmatrix} 1 & 0 & 0 \\ -0.1450 & -3,1080 \cdot 10^{-6} & 0.0245 \\ -83.5812 & 8.3285 \cdot 10^{-7} & 83.5960 \end{bmatrix} \tag{5.5}$$

which has full rank, i.e the system is observable. The controllability matrix is found to be

$$Co = \begin{bmatrix} -3,4560 & 0,5011 & 288,8565 \\ 0 & -9.2966 \cdot 10^{7} & 2.4906 \cdot 10^{7} \\ 0 & -0,4247 & -1450,1170 \end{bmatrix} \tag{5.6}$$

having full rank. The system is therefore controllable as well.

The initial parameters of the wighting functions Q and R are chosen arbitrarily. The next task is then to simulate to check whether the results correspond with the expected performance. After an iterative study while changing Q and R values, the following weighting matrices were chosen:

$$Q = \begin{bmatrix} 100 & 0 & 0 \\ 0 & 0 & 0 \\ 0 & 0 & 100 \end{bmatrix} \tag{5.7}$$

The control weight of the performance index R was set to 1.

The chosen values in Q will result in a relatively large penalty of the states x_1 and x_3. This means that if x_1 or x_3 is large, the large values in Q will amplify the effect of x_1 and x_3 in the optimization problem. Since the optimization problem are to minimize J, the optimal control u must force the states x_1 and x_3

to be small (which make sense physically since x_1 and x_3 represent the of the perturbations in rotor and generator speed, respectively). On the other hand, the small R relative to the max values in Q involves very low penalty on the control effort u in the minimization of J, and the optimal control u can then be large. For this small R, the gain K can then be large resulting in a faster response.

Since the system has been found to be observable the estimator poles can be arbitrarily placed. Hence, the poles were chosen to be at -10, -30, and -50 yielding the estimator gain matrix

$$K = \begin{bmatrix} 17,235 \\ 1.41 \cdot 10^8 \\ 89.626 \end{bmatrix} \tag{5.8}$$

The disturbance state estimator gain K_D is a scalar and chosen to 10.

It was found when doing these simulations and checking the results, that an exponential LQR were more appropriate for the current application. The exponential LQR gain were found by applying the code:

```
P=are(A+alpha*eye(3),inv(R)*B*B',Q);
Gdac=inv(R)*B'*P;
```

where alpha is the exponential time-constant chosen to 4. This resulted in the gain matrix:

$$Gdac = \begin{bmatrix} -18.2087 & -1.2265 \cdot 10^-5 & -0.0425 \end{bmatrix} \tag{5.8}$$

Simulation of the time response of perturbations in rotor speed for ten seconds is shown in Figure 5.5.

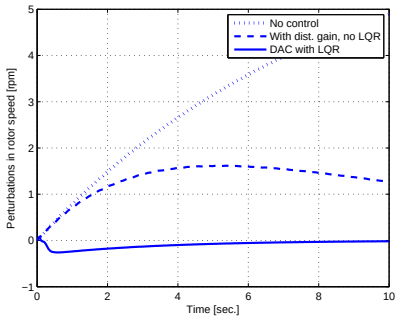

Figure 5.5: Comparison of perturbations in rotor speed when applying DAC with LQR

When looking at the plots in Figure 5.5, it is clear that the disturbance now is much better attenuated while comparing with the first two scenarios. The reason why the speed have this undershoot is due to the right complex plane zeros the LQR controller gives to the closed loop system.

It is also of interest to see how the control signal changes in the three previous situations. This is shown in Figure 5.6.

As can be seen from Figure 5.6 does the pitch angle end up having a higher value. This is an expected situation since it is now assumed a constant wind disturbance which must be accounted for by an increase

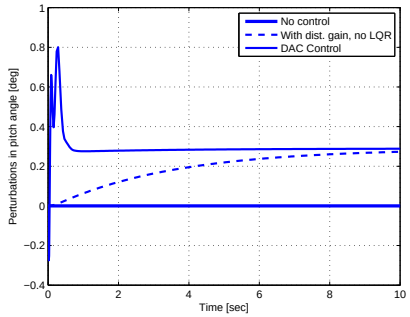

Figure 5.6: Comparison of control signal for three previous scenarios

in pitch angle. Otherwise, the step in the wind would result in a higher rotor speed, a situation we do not want to occur and the very reason for having a control system in the first place.

Another interesting signal is the error signal, which is the discrepancy between the "measured" output signal y and the estimated signal $\hat{y}$. This is shown in Figure 5.7 below.

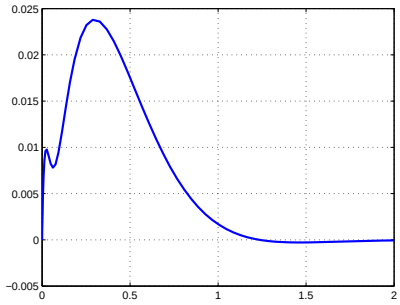

Figure 5.7: Error signal for a step input

The DAC simulations in this section have shown that this control method enables to mitigate disturbance due to a wind assigned to affect the rotor state. However, the simulations show that the settling time is relatively long (approximately 10 sec). Whether it is possible to obtained a "better" result using a LQG controller, will be the task in the following section.

The disturbance will now be replaced by two step functions and the disturbance vector Γ in order to make the DAC more comparable with the LQG analysis. This gives the disturbance input signal as shown in Figure 5.9.

The output response when applying this disturbance model is given in Figure **??**

5.4 Simulation of LQG Controller

The Simulink block diagram of the LQG, with reference to the equations presented in Chapter 4, is shown in Figure 5.10.

The control objective is the same as for the DAC; make the perturbations in the rotor speed as small as possible in order to attenuate the wind disturbance. The wind disturbance is made by using the combination

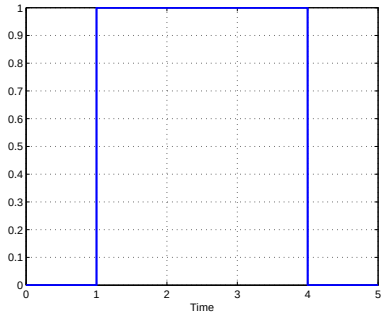

Figure 5.8: Step signal for disturbance modeling

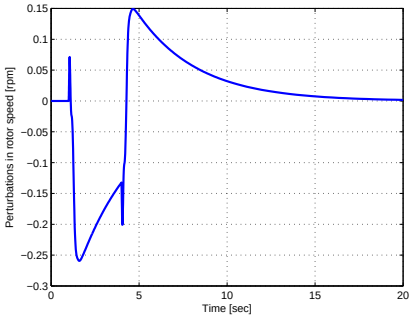

Figure 5.9: Output response when applying step input in Figure 5.9

of two step functions as described earlier. This will give a step input affecting the rotor state.

Firstly, a situation without control is showed in Figure 5.11.

The sudden change in the rotor speed after one second is due to the step input function. The figure show that without any control will the rotor speed increase to approximately 2 rpm above the operational speed. After four seconds, when the disturbance is set to zero again, will the speed then decrease and be brought to zero after approximately 50 seconds.

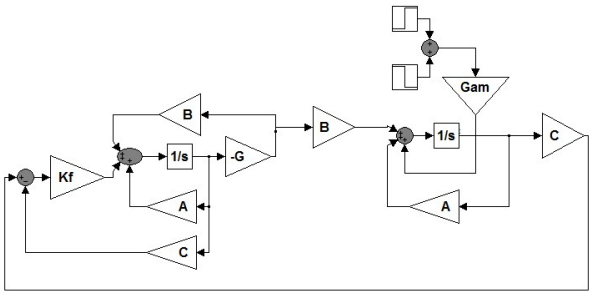

Figure 5.10: Simulink block diagram of the LQG set-up

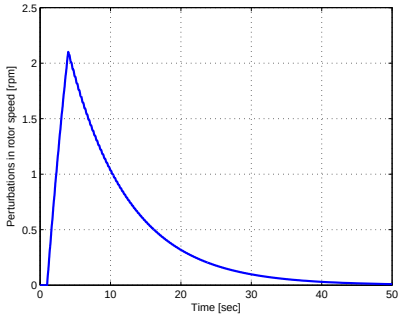

Figure 5.11: Response in rotor speed without any control

5.4.1 Kalman Gain Calculation

Calculation of the Kalman gain used in the LQG controller is according to the theory discussed in Chapter 4. There are different methods to do this calculation in MATLAB. One is by applying the `kalman` function, and another is the `lqrc` function. The latter is for instance used in the LTR demo provided with the Robust Control Toolbox in MATLAB. When applying the same weighting as for the LQR in the DAC approach in the `lqrc` function, and the weighting functions

$$Q_n = \begin{bmatrix} 30 & 0 \\ 0 & 30 \end{bmatrix}$$

R_n=1

representing the process and measurement noise covariances in the `kalman` function, did the `kalman` function yield much better disturbance attenuation for a given control effort (shown in Figure 5.12). The corresponding load attenuation for the two cases is shown in Figure 5.13 below

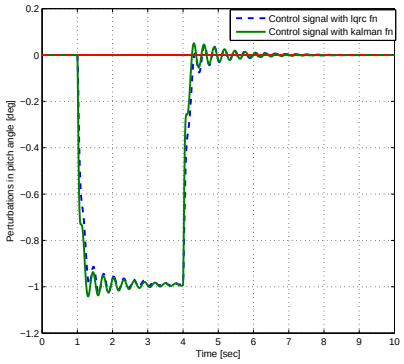

Figure 5.12: Comparison of control effort while applying `kalman` and `lqrc` functions in MATLAB

The differences in the output response can be seen through the Kalman gain matrix, which when using the `lqrc` function were calculated to

$$\mathrm{Kf} = \begin{bmatrix} 10.38 \\ -1.76 \cdot 10^{-6} \\ -1.65 \end{bmatrix} \tag{5.8}$$

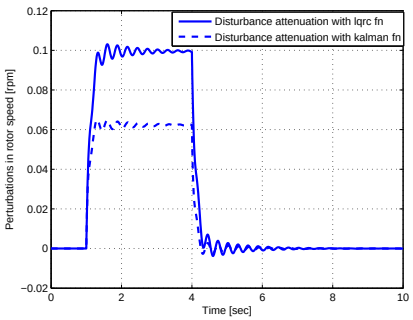

Figure 5.13: Comparison of rotor speed for similar control effort while applying `kalman` and `lqrc` functions in MATLAB

Similarly, the Kalman gain matrix when using the `kalman` function is

$$\text{Kf2} = \begin{bmatrix} 57.60 \\ 3.87 \cdot 10^{-6} \\ 1.07 \end{bmatrix} \tag{5.8}$$

5.4.2 LQR Gain Calculation

The LQR gains were calculated with an exponential LQR with a time-constant α set to 10, and were given as

$$G = \begin{bmatrix} -25.78 & -2.68 \cdot 10^{-5} & -5.70 \end{bmatrix} \tag{5.8}$$

The MATLAB script used when calculating the above gains is given in the Appendix.

5.4.3 LQG and DAC Comparison

The perturbation in rotor speed when comparing the LQG with the DAC response is shown in Figure 5.14.

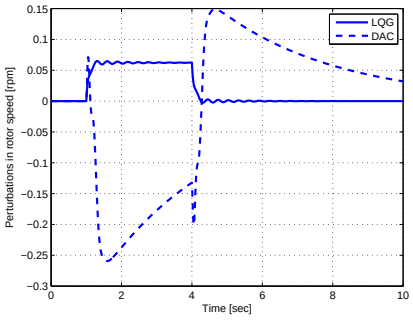

Figure 5.14: Comparison of perturbations in rotor speed for LQG and DAC

Figure 5.14 makes it clear that the effect of the two different control methods is quite different when comparing the two output signals. The LQG controller will not force the disturbance to zero in the same way as the

DAC does, which must be regarded as a disadvantage of the LQG. However, the DAC gives a much larger overshoot which is not very positive seen from a controller's perspective.

Similarly, the perturbations in pitch angle for the two methods is shown in Figure 5.15.

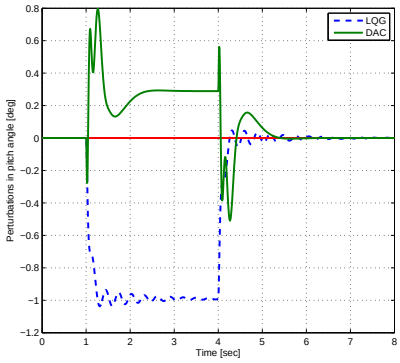

Figure 5.15: Comparison of perturbations in pitch angle for the LQG and DAC

This figure shows that the control effort is much higher for the DAC approach than for LQG. To improve the robustness properties of the LQG will the LTR approach now be introduced as a way to ensure good robustness in spite of uncertainties in the plant model.

5.5 Dynamic Controller from the LQG/LTR Algoritm

The evidence of gain an phase margin recovery can be seen in the frequency domain as shown in Chapter 4. But one important question which arises is: Can the LQG/LTR approach improve response seen in the time domain and hence increase the performance in terms of load mitigation? To answer this question it is necessary to build a new model having the dynamic state controller provided from the LQG/LTR algorithm in a feedback loop as shown in Figure 5.16

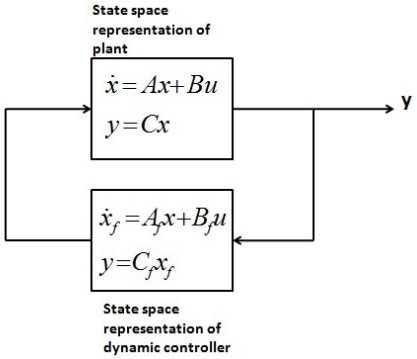

Figure 5.16: Illustration of plant and dynamic state-space controller

The matrices A_f, B_f, and C_f are extracted by using the function `ssdata(`ss_f`)` where ss_f is the state-space system of the dynamic controller from the LTR algorithm (see Appendix for more details). The Simulink set-up is shown in Figure 5.18.

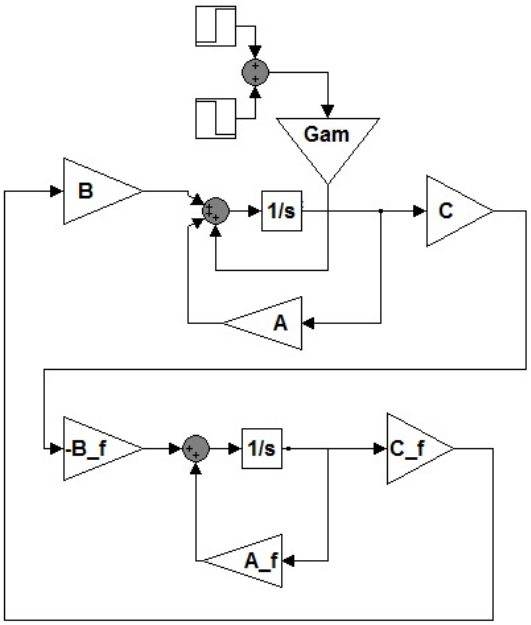

Figure 5.17: Simulink block diagram of the dynamic controller from the LTR procedure

Now, when simulating with the same disturbance as with the LQG, and comparing with these results, Figure 5.18 shows that the perturbations in rotor speed is more suppressed in the case when using the dynamic controller than with the LQG regulator.

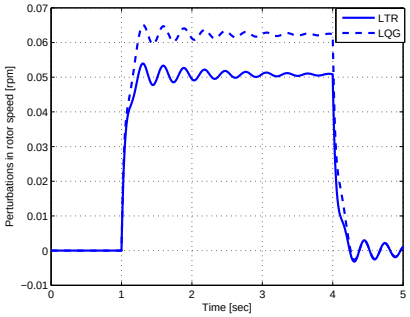

Figure 5.18: Comparison of rotor speed using LQG and LTR

However, it is important to see if the improved regulation of the rotor speed as shown in Figure 5.18 occur at the expense of increased control effort. Figure 5.19 shows that the control input signal is very similar in the the cases.

As has already been described is one of the major benefits from the LTR synthesis is how it enables to recover the lost robustness properties due to observer implementation. This can be seen in the frequency domain where the bandwidth is increased and thus allow for a more robust system in terms of stability for a wider range of disturbance levels. Whether this is true in the case of the current application will be analyzed by increasing the disturbance gain matrix.

The results from the simulations when increasing the disturbance gain matrix Γ are summed up in Table 5.1.

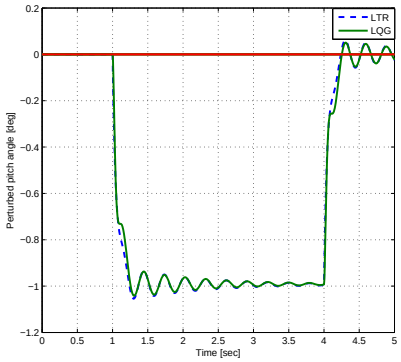

Figure 5.19: Comparison of pitch angle input

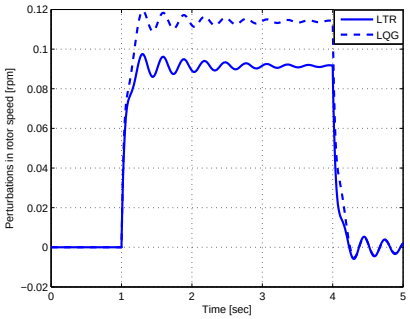

Figure 5.20: Comparison of rotor response with disturbance gain matrix set to [2;0;0]

Table 5.1 show that when increasing Γ the dynamic controller from the LTR algorithm does have less increase in output value than what is the case for the LQG. This can be regarded as an advantage of the LTR compared to the LQG.

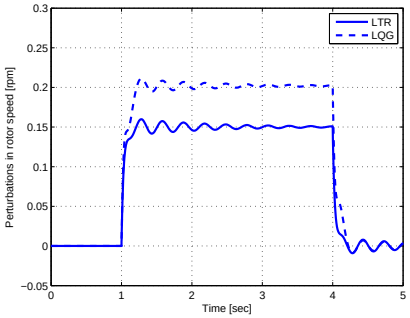

Figure 5.21: Comparison of rotor response with disturbance gain matrix set to [5;0;0]

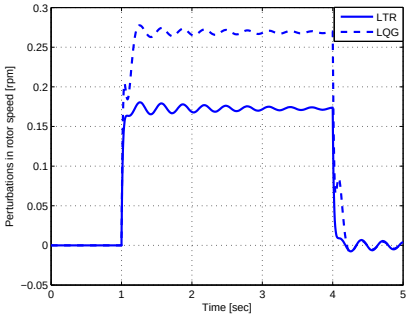

Figure 5.22: Comparison of rotor response with disturbance gain matrix set to [10;0;0]

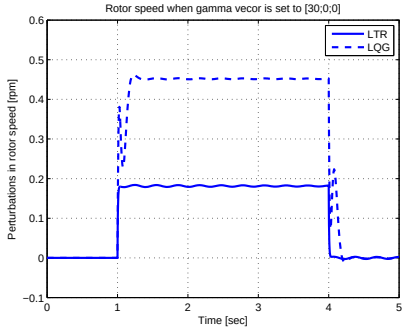

Figure 5.23: Comparison of rotor response with disturbance gain matrix set to [30;0;0]

Table 5.1: Comparison of LTR and LQG for different Γ. Values are given as approx. average values

Γ	LTR	LQG	LTR in % of LQG
$[1\ 0\ 0]^T$	0.051	0.063	81%
$[2\ 0\ 0]^T$	0.09	0.115	78%
$[5\ 0\ 0]^T$	0.15	0.21	71%
$[10\ 0\ 0]^T$	0.17	0.27	62%
$[30\ 0\ 0]^T$	0.18	0.45	40%

Chapter 6

Conclusions and Further Works

The purpose of this thesis has been to reduce the loads on a WT for above rated wind speeds (Region III) by speed control when applying different controlling methods. This was first performed by pitch regulation with DAC. This regulation policy showed to have some regulation capacity, but also resulted in some bias in the control signal. It was found when utilizing the DAC controller that although the wind disturbance was well mitigated, the settling time was relatively long(approx. 10 sec). It could have been interesting to extend the work also to include torque regulation in below rated wind speeds. This regulation policy would aim at mitigation of speed and torque variations due to wind disturbances in Region II.

The LQG regulator showed to give good speed attenuation, but since DAC and LQG is quite different approaches were a comparison between them not possible. However a comparison between the LQG and the dynamic controller extracted from the LTR algorithm showed that the LTR yielded better results in terms of speed attenuation than the LQG. Especially were this evident when increasing the disturbance gain matrix Γ. It would have been of major interest to extend the work to also considering pitch actuator constraints to see how this would have affected the results, especially the control input signal.

The lack of a non-linear simulation model and a multi-body simulation model showed to limit the application of the controllers. The problem with the simple linear state space model used is that this model only is valid with small deviations from the operating point around which the linearization is performed. It could have been of major interest, however, to see how the controller would work under other operating conditions as well. This is the reason why simulation codes as FAST can be interfaced with Simulink, which enables the control designer to use the rather complex non-linear equations of motion from FAST in an S-Function in the simple block diagram approach of Simulink, which increases the flexibility of the control integration a lot. Unfortunately, due to the limited resources available when it comes to supervision on FAST, an application of the program in this work has not been achievable.

Bibliography

[1] Fernando Vanegas A. and Carlos Zamacona. *Robust Control Solution of a Wind Turbine*. Master Thesis at Halmstad University, 2008.

[2] Adel Ben Abdennour, Rizk M. Hamouda, and A.A Al Ohaly. Countermeasures for self-excited torsional oscillations using reduced order robust control approach. *IEEE Transactions on Power Systems*, Vol. 15(No.2):pp. 779–784, May 2000.

[3] Dan Ancona and Jim McVeigh. Wind turbine - materials and manufacturing fact sheet, Princeton Energy Resources Int.

[4] Cristina L. Archer and Mark Z. Jacobson. Evaluation of global wind power. *Journal of Geophysical Research*, Vol. 110:p. 17, 2005.

[5] American Wind Energy Association. Wind energy fast facts, http://97.74.195.121/newsroom/pdf/fastfacts.pdf, 17.02.2011.

[6] World Wind Energy Association. http://www.wwindea.org, 16.02.2011.

[7] Michael Athans. The Linear Quadratic LQR problem. *Massachusets Institute of Technology*, 1981.

[8] M.J. Balas, Y.J Lee, and L. Kendall. Disturbance tracking control theory with application to horizontal axis wind turbines. *Proceeding of the 1998 ASME Wind Energy Symposium, Reno, Nevada, 12-15 January*, pages 95–99.

[9] F.D. Bianchi, R.J. Mantz, and C.F. Christiansen. Power regulation in pitch-controlled variable-speed WECS above rated wind speed. *Renewable Energy*, Vol. 29(No. 11):pp. 1911–1922, September 2004.

[10] E. A. Bossanyi. The design of closed loop controllers for wind turbines. *Wind Energy*, Vol.3:pp.149–163, 2000.

[11] E. A Bossanyi. Individual blade pitch control for load reduction. *Wind Energy*, Vol. 6:pp.119–128, 2003.

[12] E. A Bossanyi. Developments in individual blade pitch control. *2004*, EWEA conference; The Science of Making Torque from Wind DUWIND Delft University of Technology April 19-21 2004.

[13] C. Bottasso, A. Croce, and B Savini. Performance comparison of control schemes for variable-speed wind turbines. *Journal of Physics: Conference Series 75, The Science of Making Torque from Wind*, 2007.

[14] C.L Bottasso and A Croce. Cascading kalman observers of structural flexible and wind states for wind turbine control. Technical report, Dipartimento di Ingegneria Aerospaziale, Politecnico di Milano, Milano, Italy, 2009.

[15] C.L. Bottasso, A. Croce, D. Devecchi, and C.E.D. Riboldi. Multi-layer control architecture for the reduction of deterministic and non-deterministic loads on wind turbines. 2010.

[16] Encyclopedia Britannica. Retrieved from http://www.britannica.com/ebchecked/media/125134/components-of-a-wind-turbine, 04.05.2011.

[17] Liebst B.S. A pitch control system for the KaMeWa Wind Turbine. *Journal of Dynamic Systems and Control*, Vol. 107(No.1):pp.46–52, 1985.

[18] Roland S. Burns. *Advanced Control Engineering.* Butterworth Heinemann, 2001.

[19] Connor, Iyer, Leithead, and Grimble. Control of a horizontal axis wind turbine using H-infinity control. In *First IEEE Conference on Control Applications*, pages 117–122, 1992.

[20] Dataforth Corporation. Wind turbines today. 2009.

[21] A Croce and C.L Bottasso. Power curve tracking with tip speed constraint using LQR regulators. Technical report, Dipartimento di Ingegneria Aerospaziale, Politecnico di Milano, Milano, Italy, 2009.

[22] D.-W.Gu, P.Hr.Petkov, and M.M. Konstantinov. *Robust Control Design With MATLAB.* Springer, 2005.

[23] David A. Spera (Editor). *Wind Turbine Technology.* Asme Press, 1998.

[24] Tommy Ekelund. *Modeling and Linear Quadratic Optimal Control of Wind Turbines.* PhD thesis, Chalmers University of Technology, Gothenburg, Sweden, 1997.

[25] A. S. Elliot and A. D Wright. Adams/wt: An industry-specific interactive modeling interface for wind turbine analysis. *Wind Energy*, 2004.

[26] David G. Wilson et. al. Active aerodynamic blade control design for load reduction on large wind turbines. *AWEA Wind Power Conference*, 2009.

[27] David G. Wilson et. al. Combined individual pitch control and active aerodynamic load controller investigation for the 5mw upwind turbine. *AWEA Wind Power Conference*, 2009.

[28] Gary Balas et.al. *Robust Control Toolbox 3 - Getting Started Guide.* The MathWorks Inc, 2011.

[29] Iulian Munteanu et.al. *Optimal Control of Wind Energy Systems - Towards a Global Approach.* Springer - Verlag London, 2008.

[30] EU Directorate-General for Energy. *Energy 2020 - A strategy for competitive, sustainable and secure energy.* Publications Office of the European Union, 2011.

[31] Partnerships for Renewables. http://www.pfr.co.uk/standfordhill/15/wind-power/119/capacity-factor/, 06.04.2011.

[32] M. Maureen Hand. Mitigation of wind turbine/vortex interaction using disturbance accommodating control. Technical report, National Renewable Energy Laboratory, 2003.

[33] Martin O.L Hansen. *Aerodynamics of Wind Turbines.* James and James, 2000.

[34] Erich Hau. *Wind Turbines: Fundamentals, Technologies, Application, Economics.* Springer, 2000.

[35] Lars Christian Henriksen. Model Predictive Control of a Wind Turbine. *Informatics and Mathematical Modelling - Technical University of Denmark*, 2007.

[36] Grant Ingram. Wind turbine blade analysis using the Blade Element Momentum method. 2005.

[37] National Instruments. http://zone.ni.com/devzone/cda/epd/p/id/6272, 25.05.2011.

[38] C. D Johnson. Theory of Disturbance- Accommodating Controllers. *Advances in Control and Dynamic Systems*, Vol. 12:pp. 387–489, 1976.

[39] H. Karimi-Davijani, A. Sheikholeslami, H. Livani, and M. Karimi-Davijani. Fuzzy logic control of doubly fed induction generator wind turbine. *World Applied Sciences Journal*, Vol. 6 (4):pp. 499–508, 2009.

[40] Matthew A. Lackner and Gijs A. M. van Kuik. The performance of wind turbine smart rotor control approaches during extreme loads. *Journal of Solar Energy Engineering*, Vol. 132(No.1), 2010.

[41] Jason H. Laks, Lucy Y. Pao, and Alan D. Wright. Control of wind turbines: Past, present, and future. *University of Colorado at Boulder, USA*, 2009.

[42] Ching-Hung Lee. Stabilization of nonlinear nonminimum phase systems: Adaptive parallel approach using recurrent fuzzy neural network. Vol. 34(No. 2):pp. 1075–1088, April 2004.

[43] Jinho Lee and Suduk Kim. Wind power generations impact on peak time demand and on future power mix. *Green Energy and Technology*, 3:108–112, 2010.

[44] J. Gordon Leismann. Challenges in modeling the unsteady aerodynamics of wind turbines. *21st ASME Wind Energy Symposium and the 40th AIAA Aerospace Sciences Meeting*, pages 5–6.

[45] Ji-Hong Liu, Da-Ping Xu, and Xi-Yun Yang. Multi-objective power control of a variable speed wind turbine based in h infinite theory. In *International Conference on Machine Learning and Cybernetics*, 2008.

[46] J.F. Manwell, J.G McGovan, and A.L. Rogers. *Wind Energy Explained, Theory Design and Application, 2nd edition.* John Wiley and Sons, 2009.

[47] J. M. Jonkman M.L. and Buhl. Fast's user guide. *National Renewable Energy Laboratory*, 2005.

[48] P.J. Moriarty and A.C. Hansen. Aerodyn theory manual. Technical report, National Renewable Energy Laboratorium, 2005.

[49] Hiroaki Morimoto. Adaptive LQG regulator via the Separation Principle. *IEEE Transactions on Automatic Control*, VOL. 35(No. I):85–88, January 1991.

[50] Stuart Nathan. theengineer: http://www.theengineer.co.uk/in-depth/the-big-story/offshore-giants-the-rise-of-the-towering-turbine/1002898.article, 23.02.2011.

[51] Aeroservoelasticity of Wind Turbines. *Bjarne Skovmose Kallesoe.* PhD thesis, Technical University of Denmark, 2007.

[52] Ali Saberi, Ben M. Chen, and Peddapullaiah Sannuti. *Loop Transfer Recovery, Analysis and Design.* Springer, 1993.

[53] Mattson S.E. *Modeling and Control of Large Horizontal Axis Wind Power Plants*. PhD thesis, Lund Institute of Technology, Lund, Sweden, 1984.

[54] Kausihan Selvam. Individual pitch control for large scale wind turbines, 2007.

[55] Henrik Stiesdal. Wind turbine components and operation. *Bonus Energy AS*, 1999.

[56] Herbert J. Sutherland. On the fatigue analysis on wind turbines. *Sandia National Laboratories*, 1999.

[57] Huan-Liang Tsai. Generalized linear quadratic gaussian and loop transfer recovery design of f-16 aircraft lateral control system. *Engineering Letters*, Vol. 14(No.1 (Online version)), 2007.

[58] Emily Waltz. Offshore wind may power the future. *Scientific American*, October 2008.

[59] David G. Wilson and Dale E. Berg et al. Active aerodynamic blade control design for load reduction on large wind turbines. In *European Wind Energy Conference and Exhibition, 16-19 March*, 2009.

[60] A. D Wright. Modern control design for flexible wind turbines. Technical report, National Renewable Energy Laboratory, 2004.

[61] A. D. Wright and L. J. Fingersh. Advanced control design for wind turbines part i: Control design, implementation, and initial tests. Technical report, National Renewable Energy Laboratory, 2008.

[62] Alan Wright and Karl A Stol. Designing and testing controls to mitigate dynamic loads in the controls advances research turbine. *Conference Paper 2008 ASME Wind Energy Symposium*, 2008.

List of Figures

Appendix

MATLAB Script used in the Report

```
clear all
clc

A=[-0.145 -3.108*10^-6 0.0245;2.69*10^7 0 -2.69*10^7;0.1229 1.56*10^-5 -
0.229];
B=[-3.456;0;0];
C=[1 0 0];
D=0;
H=0;
Gam=[1;0;0];
Q=[100 0 0;0 0 0;0 0 100];
R=[1];
Theta=[1];
F=[0];

%%%Calculating observability and controllability matrices
Ob=obsv(A,B);
Co=ctrb(A,C);

%%%Extracting the state space system
SYS=ss(A,B,C,D)
[num,den]=ss2tf(A,B,C,D);
G_s=tf(num,den) %Plant TF

%%%Calculate kalman filter gain
SYS2=SS(A,[B Gam],C,[D H]);
Qn=[30 0;0 30];
Rn=1;
[KEST,Kf2,P] = kalman(SYS2,Qn,Rn)

%%%------------------
%%%Alternative method kalman calculation
XiTh = diagmx(Q,R)          % Put Q and R into comp. form
[Kf] = lqrc(A',C',XiTh);    % Solve Kalman filter gain
Kf = Kf';                   % Using duality with LQR
%%%------------------

%%% Exponential LQR, DAC
alphaD=4;
P=are(A+alphaD*eye(3),inv(R)*B*B',Q)
Gdac=inv(R)*B'*P;

%%% Exponential LQR, LQG
alpha=10;
P=are(A+alpha*eye(3),inv(R)*B*B',Q)
G=inv(R)*B'*P;

%Disturbance gain
G_D=-inv(B'*B)*B'*Gam*Theta %% minimize the norm

%Estimator gains
K=place(A',C',10*[-5 -1 -3])';
K_D=10;

%%% LTR algoritm (Using ltry fn)
```

```
RHO=[1e3,1e6,1e9,1e12]; %LTR gains
w=logspace(-2,2);
[re,im] = nyquist(A,Kf2,C,0,1,w); % Compute Nyquist plot
lenw = length(w);              % length of w
svk = [[re;re(lenw:-1:1,:)] [im;-im(lenw:-1:1,:)]];
                                % Pack frequency response
[ss_f,svl] = ltry(SYS,Kf2,Q,R,RHO,w,svk); % LQG/LTR at output y
[Af,Bf,Cf,Df] = ssdata(ss_f);

%%%------------------
%%%Alt. method using 'ltrsyn' and gains from 'lqrc' func
[LTR,SVL,W1]=ltrsyn(SYS,Kf,Q,R,RHO,w,'OUTPUT');
[Af2,Bf2,Cf2,Df2] = ssdata(LTR);
%%%------------------
```